Energy & Buildings 312 (2024) 114218

Contents lists available at ScienceDirect

Energy & Buildings

journal homepage: www.elsevier.com/locate/enb

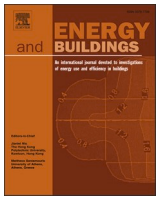

Advancing sustainable construction through comprehensive analysis of thermal, acoustic, and environmental properties in prefabricated panels with recycled PET materials

Silvia Cavagnoli [a], Claudia Fabiani [a,b,*], Fabiana Frota de Albuquerque Landi [a,c], Anna Laura Pisello [a,b,*]

[a] EAPLAB at CIRIAF - Interuniversity Research Centeron on Pollution and Environment "Mauro Felli", University of Perugia, Via G. Duranti 67, Perugia, 06125, Italy
[b] Department of Engineering, University of Perugia, Via G. Duranti 93, 06125 Perugia, Italy
[c] Norwegian Institute for Sustainability Research (NORSUS), Stadium 4, 1671 Kråkerøy

ARTICLE INFO

Keywords:
Waste material
Prefabricated
Thermal property
Acoustic property
Numerical analysis
Life Cycle Assessment
Sustainability
PET

ABSTRACT

Acoustic and thermal insulation materials play a crucial role in the construction industry as they ensure high-performance applications. This study analyzes three recycled insulations (two derived from PET and one is EPS with graphite additives) for innovative prefabricated panels. A multiphysics, multiscale, and multiobjective approach was developed to analyze the performance of the individual materials and three prototype prefabricated panels incorporating them, combined with numerical analysis enabling the thermal transmittances assessment of a full-scale panel. Thermal investigations were conducted at both small and large scales to assess their performance. Additionally, acoustic sound insulation measurements at both scales and a LCA analysis were carried out. Thermal conductivity of the insulation layer ranges from 0.026 to 0.043 $Wm^{-1}K^{-1}$. Furthermore, the sound transmission loss exhibits a positive trend with increasing frequencies, reaching approximately 10 dB after 1600 Hz for the 15 cm thick PET insulation. EPS performs exceptionally well at low frequencies, with sound insulation peaks reaching almost 40 dB around 400 Hz. At the large scale, the weighted sound reduction index showed a 3.5 dB increase compared to the reference. The environmental assessment emphasized that 80 % of global warming potential comes from material extraction, stressing the importance of using recycled materials.

1. Introduction

In recent times, global temperatures have risen year by year, leading to radical changes in our environment. One of the main causes of these phenomena is global warming triggered by the increase of greenhouse gases in the atmosphere, which have a negative effect on both the energy balance of our planet and human life on earth. Because of climate change, different types of phenomena have developed such as melting glaciers and thawing permafrost with an estimated loss of several billion tonnes of ice in recent decades and rising sea level, which is estimated to increase progressively in the future.

In addition to these interconnected natural phenomena, anthropogenic activities also have a negative effect on the environment and, in particular, the construction activity is one of countless causes of the environmental decline [1]: the global status report for buildings and construction [2] states that the construction sector is responsible for about 39 % of the total carbon dioxide emissions and for about 36 % of the total energy use worldwide. In this view, the building sector is constantly trying to develop new strategies to achieve very high performance with minimal consumption and emissions. Materials' selection and optimization, in particular, is of paramount importance in building design and should be carried out by choosing the most appropriate solutions to meet at the same time the demands of low energy consumption also affected by final energy uses [73], low impact on the environment, and high performance especially in thermal, acoustic, and sustainability terms. To this end, there are different studies that analyze the thermal and acoustic properties of materials or panels in order to meet indoor wellness requirements. Some of these studies aim at evaluating the performance of panels characterized by reinforcing materials with nonwoven fabrics [3], panels made of wood with an inner layer made of polyurethane [4], or panels made of recycled waste materials [5,6]. Indeed, the use of recycled materials offers numerous benefits, such as

* Corresponding authors at: CIRIAF - Interuniversity Research Center, University of Perugia, Via G. Duranti 67, 06125 Perugia, Italy.
E-mail addresses: claudia.fabiani@unipg.it (C. Fabiani), anna.pisello@unipg.it (A.L. Pisello).

https://doi.org/10.1016/j.enbuild.2024.114218
Received 20 December 2023; Received in revised form 23 April 2024; Accepted 27 April 2024
Available online 28 April 2024

minimizing the amount of waste sent to landfills, mitigating environmental impacts, and lowering expenses associated with their disposal. A study conducted by Hossain et al. shows how some materials from construction and demolition (C&D) waste can actually be reused in different ways with a significant reduction in greenhouse gas emissions and nonrenewable energy consumption [7]. Indeed, there is the potential to discover new applications for various materials like discarded tires [8], roof tiles [9], glass [10], plastic [11], and even manure [12]. These materials can be repurposed effectively in the construction of concrete elements, for paving, infrastructure development, and various other engineering applications [12]. Specifically, the production of plastic has witnessed a significant rise in recent times owing to its convenience and widespread usage in daily life. Everyday items such as plastic bags at supermarkets, plastic bottles, toys, and food containers exemplify this trend. However, this progressive surge in production has also resulted in a corresponding increase in plastic waste, posing a considerable environmental challenge. Indeed, researchers are studying methods to reinsert this waste into production processes. For instance, the use of these materials for road construction [11], improving the viscoelastic behavior of bitumen [13], and also for the construction of concrete sidewalks has shown promise [14]. Multiple studies have examined concrete mixtures that incorporate plastic waste as aggregates. In particular, Thorneycroft's study proposes new concrete mixtures by replacing 10 % of the sand with recycled plastic [15] while the work presented by Agyeman et al. explores the use of plastic material as a binder for the production of concrete paving blocks [16]. Notably, polyethylene terephthalate (PET) plastic waste, commonly found in plastic bottles from the food industry, is a key component of plastic waste. Various studies in the literature have explored innovative approaches to reintegrate PET in different fields [17] but also in construction contexts, particularly in brick and concrete production.

Hassan et al. [18] conducted a comprehensive review of potential integration solutions for PET, examining its incorporation into the production of clay bricks or concrete bricks. Their studies primarily delved into the physical and mechanical properties of these novel materials, encompassing compressive strength, flexural strength, density, and water absorption. Similarly Limami et al. [19] conducted tests to assess the impact of introducing PET into a clay mixture, considering variations in proportions based on weight and grain size. Their analyses focused on the porosity of the resulting bricks, coupled with density analysis, capillary water absorption coefficient, and compressive strength. Comparable analyses have been performed in the literature on different types of bricks incorporating PET [20–25]. Furthermore, PET waste has been explored for its application in PET foams used in composite sandwich panels. Studies have involved various tests, including DMA, DSC/TGA, and Iosipescu tests [26], as well as assessments of bending [27], shear stiffness, thermal stability, and humidity [28]. Additionally, PET waste has been used to produce unsaturated polyester resin [29,30] acting as reinforcement for precast concrete [31] or as an additive in the production mix for precast concrete panels, with analyses focusing on rupture strength and impact resistance [32]. The versatility of PET materials extends to green roofs, where whole PET bottles are utilized in the stratigraphy of the roof [33] and [34], and in the production of panels [35], prefabricated slabs [36], and interior walls [37], accompanied by thermal tests. Furthermore, in order to follow a sustainable approach, reference can be made to the Life Cycle Assessment (LCA) study [38,39], from which different strategies and solutions can be compared in order to seek the most appropriate and sustainable one. Indeed, some literature articles developed an LCA analysis on PET panels to evaluate their environmental and ecological impacts [40,41].

In this context, in addition to the continuous search for new strategies to recycle materials, prefabricated constructions are becoming more and more popular due to new technologies that allow a lower impact on the environment. Prefabricated construction can be used in different types of buildings and reduce construction time and, consequently, energy consumption and environmental pollution. Due to these characteristics, several studies are aimed at detailed analysis to identify the greatest potential of prefabricated construction. The great functionality of precast has also allowed this technology to be used for underground stations, particularly in China [42] where precast is heavily used. A study by Lu et al [43] on the design of a hundred high-rise buildings in Hong Kong estimated a reduction of more than 15 % in waste production by simply using prefabricated construction. In addition, prefabrication has further advantages: the assembly and disassembly of components is simpler and faster, site costs are reduced, there is more control during the design phase, CO_2 emissions are lower, and it is easier to recycle elements or materials. This type of construction allows different types of materials to be implemented to produce building partitions. Indeed, it is possible to produce prefabricated wood composite panels [44], use sandwich panels with PCM [45], or even natural fibers such as bamboo [46] as a reinforcing material. Despite the numerous studies carried out on prefabricated elements, only a few focus on thermo-acoustic properties, which are essential parameters for achieving high levels of comfort in a structure. However, O'Hegarty's research examined the thermal characteristics of a slim premanufactured panel composed of two concrete layers, which included a high-performance insulating slab. The study found that this panel exhibited a lower thermal transmittance compared to a traditional precast panel [47]. On the other hand, research conducted by Peng et al. offers a comprehensive examination of a prefabricated composite panel, including thermal and acoustic analyses, revealing a heat transfer coefficient of 0.55 W/m^2K and a weighted sound pressure difference of 42 dB [48].

The predominant focus of existing research has centered on the fundamental structural properties of PET panels, crucial for their application in construction. However, beyond these structural considerations, addressing thermal, acoustic, and environmental sustainability aspects is equally vital, playing a pivotal role in enhancing building comfort and promoting energy conservation. Functional buildings must effectively control external thermal and acoustic phenomena [49], irrespective of their specific use [50,51].

Considering the limited scientific literature on the thermal and acoustic properties of prefabricated panels, this study introduces an innovative approach that amalgamates the benefits of prefabricated construction with plastic recycling, addressing the imperative to reduce carbon emissions in the construction sector. The objective is to unveil a novel prefabricated panel design incorporating recycled materials, thereby optimizing interior comfort levels and minimizing resource waste. The aim is to develop an efficient structure with a production chain in which environmentally friendly materials and recycled materials are favored and with innovative design and technology.

In this context, a widespread waste is reintroduced into a production cycle to produce a high-performance building product in all fields. In particular, an insulation using polyester fibers derived from recycled plastic bottles is analyzed in detail. In addition, an alternative type of EPS insulation is presented, enriched with graphite additives to improve performance. The resulting panel is ready to use and easy to install in a very short time.

To evaluate the properties of such panels comprehensively, a multiphysics, multiscale, and multiobjective approach was implemented. This approach involved analyzing both functional properties and environmental performance, encompassing individual components and prototype panels consisting of three distinct insulation types. The study presents thermal and acoustic results at both small and large scales, supplemented by a numerical analysis using the Finite Element Method (FEM) to assess a panel with real dimensions under different boundary conditions.

Concurrently, a Life Cycle Assessment (LCA) study was conducted to evaluate emissions throughout the panel's production cycle. This analysis considered the impact of each material and explored alternative materials, contributing a holistic understanding of the environmental implications associated with the panel's life cycle. This comprehensive

approach distinguishes our work by offering a nuanced exploration of the multifaceted aspects of prefabricated panels, emphasizing innovation in design, material selection, and environmental considerations.

2. Materials and methods

This study focuses on the production of an innovative prefabricated panel for building applications. A multiscale investigation procedure was carried out to evaluate the most important thermal and acoustic properties of the panel: individual components were analyzed at the small-scale while the multilayer prefabricated panel was tested at the large-scale under real-world conditions. Additionally, advanced numerical analyses were used to better evaluate the in-filed thermal performance of the panel and quantify the associated environmental impact.

2.1. Materials and samples

The proposed new precast panels consist of an insulating material sandwiched between two concrete slabs. Three different prototypes are produced by changing the interposed insulating material and later tested:

1. I_EPS: Expanded Sintered Polystyrene with graphite additive;
2. PET: Polyester fiber insulation from recycled plastic bottles made of polyester fiber (85 % recycled from pet);
3. EF_PET: Insulation characterized by the same properties as the previous one with evolved fibers and different density.

Specifically, I_EPS is a product that improves the performance of regular EPS and has a density of almost 17 kgm^{-3}. Indeed, graphite particles play a crucial role in mitigating the impact of heat radiation by actively impeding its transmission. Through the dual mechanisms of absorption and reflection of infrared radiation, these particles effectively enable the containment and reduction of heat-related effects, enhancing radiative trapping within the pores. Moreover, since it is a material of natural origin, helps make the final product recyclable and environmentally friendly. On the other hand, PET has a density of about 40 kgm^{-3} and EF_PET about 25 kgm^{-3}. EF_PET is composed of a specific selection of advanced fibers to improve insulation properties. Literature studies have shown that to obtain PET with better performance, pre-crystallized chips are heated to remove traces of volatiles [52]. Both have the advantage that they can be entirely reused if not nicked or damaged by external substances.

2.1.1. Small-scale samples

Two types of small-scale samples were prepared for investigating the thermal and acoustic performance of the single layers constituting the precast composite. Samples were made of PET, EF_PET and I_EPS and 3 samples per type were produced. Thermal analyses were conducted on 5-cm thick sheets with a square area of 20 cm x 20 cm (Fig. 1, left panel). As for the acoustic tests, cylindrical samples with a diameter of 10 cm were produced and tested (Fig. 1, right panel).

2.1.2. Multilayered precast panels

Three multilayered precast panels were produced and tested at the large scale. Each panel features two concrete slabs. The outer slab is 5 cm thick while the inner one is 6 cm thick. Between them, a 19 cm thick layer of the three insulation materials described in section 2.1 was interposed. Fig. 2.a shows the panel with PET insulation (MP-PET), Fig. 2.b shows the panel with I_EPS insulation (MP-EPS) and Fig. 2.c shows the panel with EF_PET insulation (MP-EFEPS). All panels have a total thickness of 30 cm and a surface area of about 1.90 m^2.

Each panel was mounted on the outer wall of a test room building located at University of Perugia (Fig. 3.a,b) in place of the security door on the North side. The test room has a square floor plan with a side of approximately 3 m (Fig. 3.c) and has an access door on the North side and a rectangular double-hung window on the South side.

3. Investigation methodology

This paper develops a multiphysics, multiscale, and multiobjective investigation procedure. In particular, the proposed panel for building applications is analyzed both from an acoustic and thermal point of view. These analyses were performed both on small-scale samples (small-scale investigation) and on the prototype panel with larger dimensions making use of a test room building for in-field testing (large-scale investigation). Additionally, a numerical thermal analysis was also conducted to evaluate the performance of the precast panels considering different boundary conditions and the environmental impact of the panels was assessed in a life cycle perspective according to the LCA methodology, presented in Section 5.

3.1. Methods for acoustic characterization

In the construction sector, the choice of specific materials is important for optimal sound insulation of a structure/building. To achieve a high level of acoustic intelligibility, it is important to protect the building from external noise (such as road and rail traffic or even just the chattering of people) with proper acoustic design, which consequently

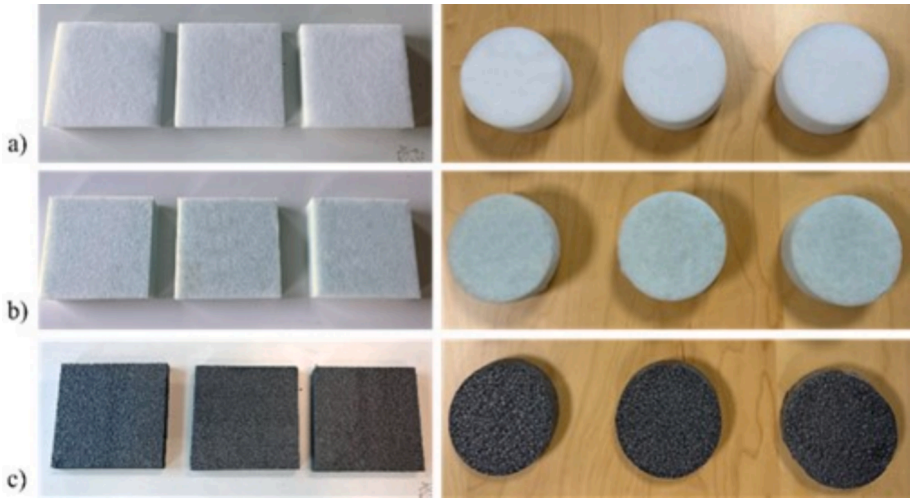

Fig. 1. (a) PET, (b) EF_PET, (c) I_EPS: Small-scale thermal test samples (left), small-scale acoustic test sample (right).

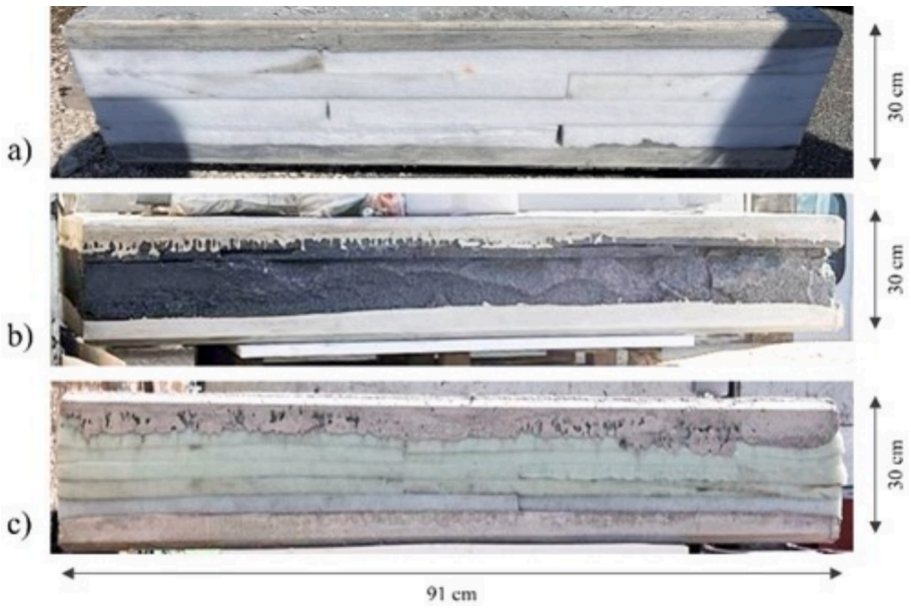

Fig. 2. MP-PET (a), MP-EPS (b), MP-EFPET (c) panels.

Fig. 3. a) Test room, b) removal stage of one of the panels, and c) facades and plan of the testroom (pictures from [53]).

leads to a positive influence on the daily life of the occupants.

3.1.1. Small-scale investigation

The small-scale characterization of the insulation materials is aimed at evaluating the acoustic insulation capability, primarily measured through achieved transmission loss (TL). This parameter was evaluated using the "two-load" transfer function method (utilizing 4 microphones) in accordance with the ASTM E2611-17 [54] and ISO 10534-2 [55] standard, by using a Brüel & Kjær impedance tube model 4206.

The impedance tube, illustrated in Fig. 4.a, consists of a loudspeaker that emits the sound wave and a sample holder where the material under examination is positioned. The loudspeaker produces plane sound waves that collide with the sample and are partially reflected or absorbed by the material, and partially penetrate through the material, ultimately reaching the receiving tube. Microphones, calibrated and placed both upstream and downstream of the sample, record the sound pressure levels. The upstream microphones capture the sound field's pressure level impacting the sample, whereas the downstream microphones gauge the pressure level on the opposite side of the sample. As part of the procedure, a background noise calibration measurement is conducted. This process involves utilizing an anechoic environment coupled with a rigid termination of the tube. Subsequently, after the insertion of the material sample, signal measurements are carried out under similar conditions, using both the anechoic and empty end of the tube, mirroring the prior setup. The process culminates in the calculation of the transfer function, enabling the quantification of the material's transmission loss. The testing employed a large tube configuration with 10 cm diameter samples, covering frequencies from 100 to 1700 Hz. Concurrently, the testing environment's temperature (°C), relative humidity (%), and atmospheric pressure (hPa) were monitored. Transmission loss assessments were carried out on samples of 5 cm, 10 cm, and 15 cm thickness. The profiles presented in Section 4.1 are averages derived from three separate tests on each sample under consistent conditions. This method was adopted to minimize potential errors stemming from individual measurements.

Table 1 shows the environmental conditions in which tests were performed for the 5-cm thickness. The environmental parameters during the tests for the other thicknesses did not deviate much from those listed.

Table 1
Environmental parameters.

Material	Temperature (°C)	Relative Humidity (%)	Pressure (hPa)
I_EPS	27.0	59	980
EF_PET	27.4	54	982
PET	27.5	54	982

3.1.2. Large-scale investigation

The large-scale acoustic characterization was carried out following the ISO 16283-3:2016 [56]. This standard prescribes the method for measuring the airborne sound insulation of facade elements in situ and it also complies with ISO 354:2003 [57], UNI EN ISO 3382-2:2008 [58], and UNI EN ISO 717-1:2021 [59]. By means of the in situ measurement of facade airborne sound insulation, it is possible to determine the evaluation index of normalized facade sound insulation with respect to reverberation time by calculating $D_{2m,nT}$ which is the standardized level difference with respect to a reference value of reverberation time in the receiving room calculated by the following Equation (1):

$$D_{2m,\ nT} = L_{1,2m} - L_2 + 10\log\left(T/T_0\right) \quad [dB] \tag{1}$$

With:

- $L_{1,2m}$ = average sound pressure level in the outdoor environment at 2 m from the facade;
- L_2 = average indoor sound pressure level;
- T = reverberation time in the receiving environment;
- T_0 = reference value of the reverberation time in the receiving environment, $T_0 = 0.5$ s.

The following instruments were used to perform the tests (Fig. 5.a-e):

- Acquisition system consisting of the Sinus Soundbook with the Samurai software to manage the various measurement phases;
- Two microphones consisting of a Random Incidence microphone capsule from GRAS and a preamplifier from 01 dB-Stell with a frequency scale of 1–20 Hz;
- Electroacoustic calibrator capable of generating a 1000 Hz signal with a sound pressure level of 94 Hz;
- LookLine omnidirectional sound source consisting of 12 speakers used for reverberation time measurements;
- Directional sound source for facade sound insulation measurements consisting of an 8″ high-efficiency loudspeaker.

To better quantify the sound insulation performance of the precast

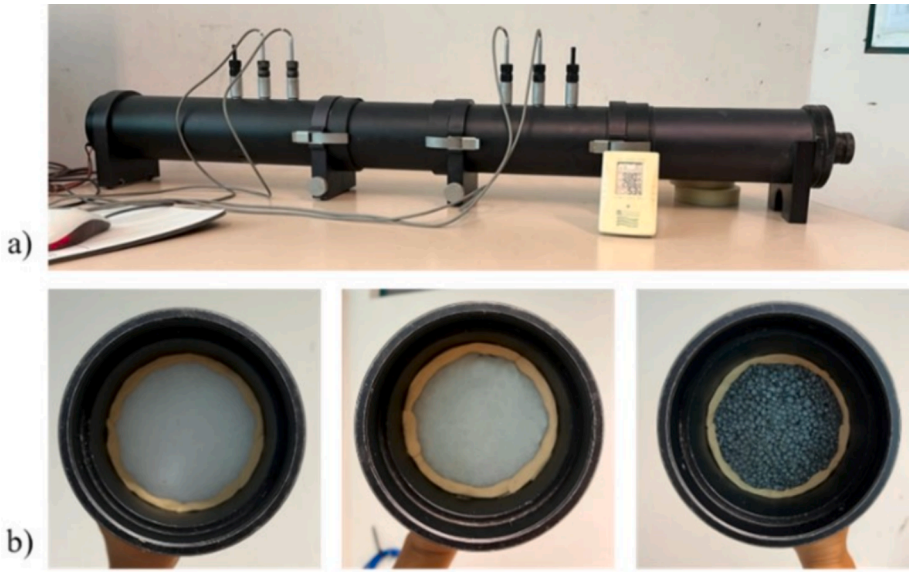

Fig. 4. a) Impedance tube, b) samples tested from left: PET, EF_PET, and I_EPS.

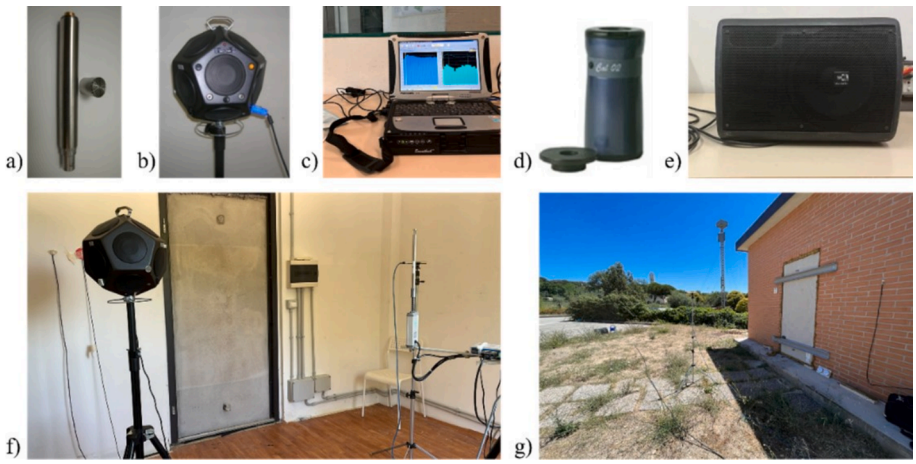

Fig. 5. a) Microphone capsule and preamplifier, b) omnidirectional sound source, c) sinus soundbook, d) electroacoustic calibrator, e) directional sound source, f) absorption test setup, and g) facade sound insulation test setup.

panel, the standardized level difference of the same test room was analyzed before and after its installation in similar local boundary conditions.

First, the temperature and relative humidity inside the test room and in the outdoor environment were assessed with two Trimtec Sistemi model Fisher 35004 thermo-hygrometers. Secondly, the reverberation time inside the room was measured by using a dodecahedral source and a calibrated microphone. During the test, the source emits a pink sound, and the microphone detects its decay once the source is switched off. The test was carried out by varying the position and height of both the sound source and the microphone.

After conducting this test, the assessment of the sound insulation of the facades was carried out. In order to do so, it was necessary to remove the dodecahedral source from inside the test room, leaving only the microphone. A directional sound source positioned outside the test chamber and facing the specific facade with the angle of sound incidence equal to $45° \pm 5°$ was utilized. During the test, the microphone inside the test chamber changed its position and height with each stress applied to the source, while another microphone was placed outside at a fixed position and height. Upon completion of the test, sophisticated software and a dedicated Excel sheet were employed to calculate the standardized level difference. The same procedure was then followed once the panel was placed in place of the entrance door on 20th July 2022 to evaluate any differences obtained in the two test configurations (Fig. 5.f,g). Table 2 shows the temperature and relative humidity conditions of the environments in which the tests were carried out.

3.2. Experimental methods for thermal characterization

In this work small and large-scale thermal analyses are used to evaluate the performance of the proposed multilayered precast panel. Small-scale analyses allowed to evaluate the performance of the different insulating layers while the large-scale investigations aimed at evaluating the overall behavior of the panel.

Table 2
Environmental conditions during acoustic test.

	INDOOR ENVIRONMENT		OUTDOOR ENVIRONMENT	
	Temperature (°C)	**Relative Humidity (%)**	**Temperature (°C)**	**Relative Humidity (%)**
Standard test room	19	54	26	33
Test room with panel	27	26	33	14

3.2.1. Small-scale investigation

The small-scale thermal measurements were carried out using a Hot Disk 2500 S equipment and the Transient Plane Source (TPS) method following the ISO 22007-2 standard [60]. The Hot Disk 2500 S (Fig. 6.a) performs a non-destructive thermal testing and characterizes each sample in terms of thermal conductivity, thermal diffusivity, and volumetric specific heat. To perform the test, a double spiral sensor/heat source is placed between two pieces of the same material characterized by a smooth surface to allow adequate thermal contact. When the test is started, the sensor generates heat that radiates into the material, causing the system temperature to rise. By analyzing this change in temperature as a function of time, the main thermal properties of the material are calculated. Before the testing process, the samples were placed in the laboratory near the instrument for one day to allow them to reach out stationary ambient condition. This ensured that the samples remained stable without experiencing any temperature fluctuations during the test. Three measurements were carried out for each sample with the bulk Isotropic module by moving the sensor to three different positions. The obtained results were later averaged, and the standard deviation was calculated. Each test was conducted using a Kapton Hot Disk 8563 probe with a radius of 9.868 mm. Fig. 6.b-d shows the samples tested.

3.2.2. Large-scale investigation

Large-scale characterization allows to evaluate the performance of the multilayered precast panel when exposed to a real environment to reproduce the actual performance in a real application. In this study, the large-scale thermal characterization was conducted through a thermo-fluximetric campaign on each panel's stratigraphy, as described in Section 2.1.2, following ISO 9869-1 [61] guidelines. The Thermozig BLE, which features two measuring nodes allowing simultaneous measurements, was used to perform the thermo-fluximetric analysis. To achieve this, temperature and fluxmeter sensors were employed. To be precise in our measurements, we placed four surface temperature sensors on the panel: two on the inner side and two on the outer side, allowing us to calculate the average and obtain more accurate results. Additionally, to avoid any interference from external climatic effects, the heat flow sensor was strategically installed on the inner side of the panel. By continuously monitoring the data collected over a significant period, we calculate the thermal transmittance (U) using Eq. (2):

$$U = \sum_{j=1}^{n} q_j / \sum_{j=1}^{n} \left(Ti_j - Te_j\right) \quad (2)$$

where j represents the number of measurements, q denotes the heat flux, Ti is the internal temperature, and Te is the external temperature. This analysis required maintaining a temperature difference between the

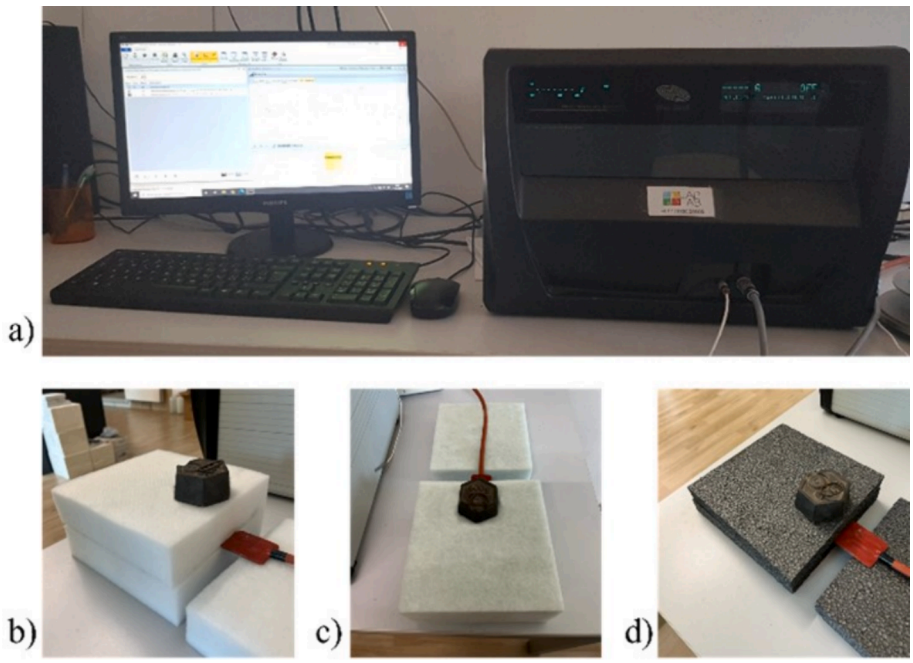

Fig. 6. a) Hot Disk 2500 s, b) PET, c) EF_PET, and d) I_EPS.

interior and exterior of the test room within the range of 1 to 20 °C. To achieve this, we conditioned the environment inside the test room to a fixed temperature of 18 °C, which represents the lowest possible temperature setting in the cooling system. Meanwhile, outside the test room, temperature fluctuations were allowed to occur naturally due to the alternation between day and night. Throughout the entire testing process, the internal temperature of 18 °C was consistently maintained to ensure reliable and consistent results. To commence the measurements, two nodes were employed to measure the relevant parameters on both the inner and outer sides of the panel. All sensors were carefully positioned in a central area of the panel, meticulously adhered to ensure precise data collection. The tests started on June 7, 2022, utilizing panels with dimensions of 91 cm x 209 cm and a thickness of 30 cm. Fig. 7 illustrates one of the three panels used in this study, showcasing the arrangement of sensors for the thermo-fluximetric analysis.

3.2.3. Numerical investigation

A comprehensive numerical simulation was employed to analyze the behavior of panels in a validated numerical environment, incorporating experimental data. This simulation allowed us to replicate and study the panels under various boundary conditions, significantly reducing the duration and complexity of certain experimental tests. Three prototype panels, as discussed in previous sections, were carefully modeled, and validated. The main objective of this modeling and validation was to assess the thermal transmittance of real panels used in construction. To achieve this, the Finite Element Method (FEM) was utilized to accurately simulate the behavior of the panels as observed in the physical test room. The aim was to precisely determine the thermal properties of the actual panels within the virtual environment. The modeling process began by replicating the geometry and characteristics of the panels, considering the dimensions described in section 2.1.2 (209 cm x 91 cm). To expedite the simulations, only half of the panel was modeled, employing a symmetry plane. Additionally, each modeled element was

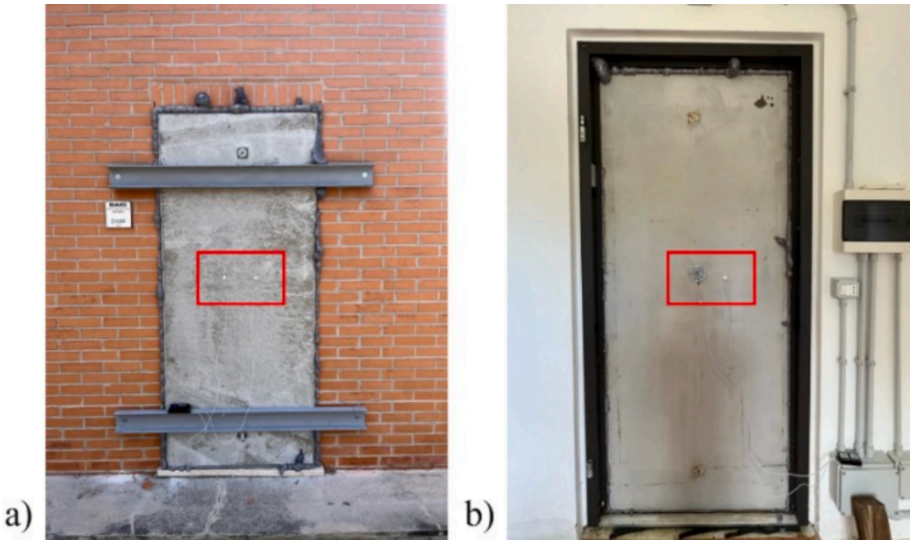

Fig. 7. External (a) and internal (b) view of one of the three panels tested with the sensors highlighted in the box.

assigned specific materials with their corresponding properties, as outlined in Table 3. The initial step involved validating the numerical model to ensure its accuracy, aiming to obtain comparable results with the experimental data collected during the monitoring in the test room.

The finite element calculation was carefully configured to consider two main aspects: heat transfer by conduction through the modeled solid materials and heat exchange by convection and radiation on the panel walls in direct contact with the internal and external air volume. For the boundary conditions, we took into account the specific days and times of the large-scale thermal monitoring of the three panels, as explained in Section 4.4. The parameters considered for each panel are the internal air temperature in the test room and the external outdoor temperature, as well as the internal and external average adduction coefficients equal to 10 $Wm^{-2}K^{-1}$ and 45 $Wm^{-2}K^{-1}$ respectively. Using these parameters, a first transient study was conducted based on the experimental thermal profiles mentioned earlier, after a stationary spin-up. This allowed us to map the thermal distribution across the entire volume of the panels and determine the heat flux passing through them. To validate the accuracy of the model, we compared the internal and external surface temperature profiles, along with the conductive heat flow, with the experimentally obtained data. By leveraging the simulation results, we calculated the thermal transmittance of each panel using Eq. (2). This comparison between experimentally derived transmittance values and those from the virtual model confirmed the validity of the panel models tested in the experimental setup.

Afterwards, a second study was conducted to evaluate the thermal transmittance of the three panels based on their actual dimensions, thereby enabling an assessment of their in-field thermal attributes. The simulation methodology paralleled the aforementioned description, yet encompassed panels measuring 815 cm × 249 cm with a 30 cm thickness. Noteworthy features comprised a 5 cm insulation layer spanning the entire height (except for the final 35 cm), supplemented by alternating 14 cm insulation and 15 cm concrete layers. Refer to Fig. 8 for a visual representation of these panel configuration. This additional stationary analysis was conducted to simulate a more substantial temperature difference between the indoor and outdoor environments than what was experienced in the large-scale tests. Specifically, we established a temperature difference of 20 °C between the inside and outside conditions. Finally, the thermal transmittance was determined to assess the panel's overall thermal performance.

4. Results and discussion from the experimental investigations

This section presents and comments on the results obtained from the analyses discussed in the above.

4.1. Small-scale acoustic analysis results

Fig. 9 displays the transmission loss value profiles for the I_EPS, EF_PET, and PET samples. In the results obtained for I_EPS insulation, a less regular trend can be seen than those obtained for the other two types of insulation. Notably, across the three thickness variations, a pronounced enhancement is evident within the initial frequency range up to approximately 600 Hz. However, an intriguing departure from mass-related behavior is observed between 600 and 1000 Hz. Here, despite escalating thickness, the transmission loss does not uniformly follow mass-related expectations. This unconventional behavior can potentially be attributed to the unique structural composition of I_EPS. Being the lightest and most rigid material among the trio, I_EPS diverges from the conventional characteristics of massive materials. Consequently, even with heightened sample thickness, the overall transmission loss does not increase as anticipated. Nevertheless, it's important to note that I_EPS outperforms the other materials in terms of transmission loss, showcasing values nearing 40 dB around 400 Hz for the thickest sample.

Looking more specifically at the other two insulators, the sound insulation of EF_PET is lower than PET. Also in this case, this could be due to their different density: PET has a density of about 40 kgm^{-3} while EF_PET has a density of about 25 kgm^{-3}. Indeed, analyzing the structure of the material, EF_PET is composed of less dense fibers than the other one, resulting in a softer material. Curiously, while I_EPS demonstrates a progressive enhancement in transmission loss performance as thickness escalates, especially within lower frequency ranges, EF_PET and PET display their strengths in higher frequencies. Furthermore, as frequency increases, both EF_PET and PET demonstrate an amplified performance, leading to prominent peaks in their transmission loss profiles. Notably, EF_PET attains peaks of nearly 9 dB, whereas PET reaches around 11 dB. This phenomenon accentuates the materials' ability to effectively mitigate sound transmission, especially at specific frequencies.

4.2. Large-scale acoustic analysis results

Moving on to our investigation of acoustic characteristics on a larger scale, the acoustic tests were conducted on both the standard test room configuration and the configuration with the added panel. In the standard test room conditions, the facade sound insulation evaluation index $D_{2m,nT}$ was determined equal to 41.7 (−2;−5) dB with $C_{100\text{-}5000} = -1$ dB and $C_{tr100\text{-}5000} = -4$ dB. Conversely, the introduction of the panel led to a notable increase in this value, reaching 45.2(−1;−3) dB with $C_{100\text{-}5000} = 0$ dB and $C_{tr100\text{-}5000} = -3$ dB. This data is visually presented in Fig. 10, offering a graphical representation of both test room setups. The graphical depiction provides clear insight into the effectiveness of the panel in significantly enhancing sound insulation when compared to the standard test room setup. This enhancement is particularly evident across the entire frequency spectrum, prominently in the lower frequencies. Noteworthy is the observation that between the frequency range of 315 Hz and 1250 Hz, there is a discernible rise in sound insulation efficacy within the standard test room configuration, maintaining a consistent level of around 40 dB.

At higher frequencies, the installation of the panel contributes to a substantial augmentation in sound insulation performance. This enhancement culminates in a distinct peak, registering an approximate value of 60 dB at 4000 Hz. The convergence of these findings underscores the considerable advancement in sound insulation achieved through the integration of the panel.

4.3. Small-scale thermal analysis results

Table 4 shows the results obtained from measurements performed on each type of small-scale sample using Hot Disk 2500 S. For each test, the values of thermal conductivity ($Wm^{-1}K^{-1}$), thermal diffusivity (mm^2s^{-1}), and volumetric specific heat ($MJm^{-3}K^{-1}$) of the three tests performed are shown, along with the corresponding average and standard deviation.

These assessments were conducted within a laboratory environment at approximately 28 °C. Upon comparing the thermal conductivity values derived from the three insulation types, the optimal performer in stationary conditions emerges as I_EPS, boasting the lowest thermal conductivity value of 0.026 $Wm^{-1}K^{-1}$. It is followed by EF_PET and PET with values of 0.0395 $Wm^{-1}K^{-1}$ and 0.043 $Wm^{-1}K^{-1}$ respectively. Turning attention to thermal diffusivity, describing a material's propensity for heat propagation, I_EPS possesses superior resistance to thermal wave propagation compared to the other materials, showcasing

Table 3
Values obtained from experimental tests carried out on small samples.

	Thermal conductivity ($Wm^{-1}K^{-1}$)	Heat capacity ($J\,kg^{-1}K^{-1}$)	Density (kgm^{-3})
Concrete	1.72	800	2442.5
PET	0.043	894	39.15
EF_PET	0.0395	936.9	24.55
I_EPS	0.026	1916.2	16.7

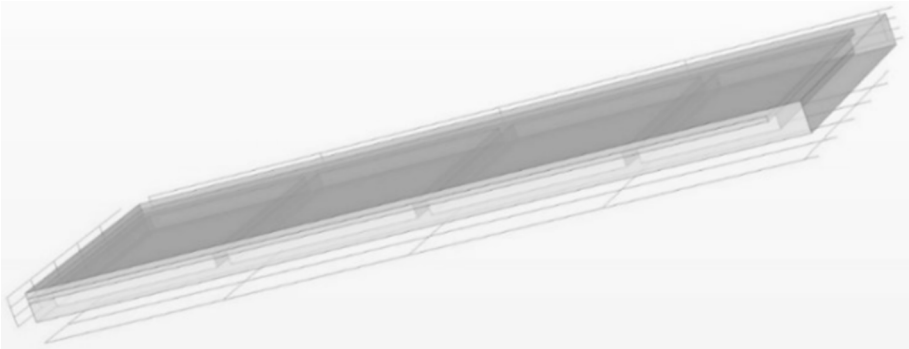

Fig. 8. Geometry panel with real dimensions.

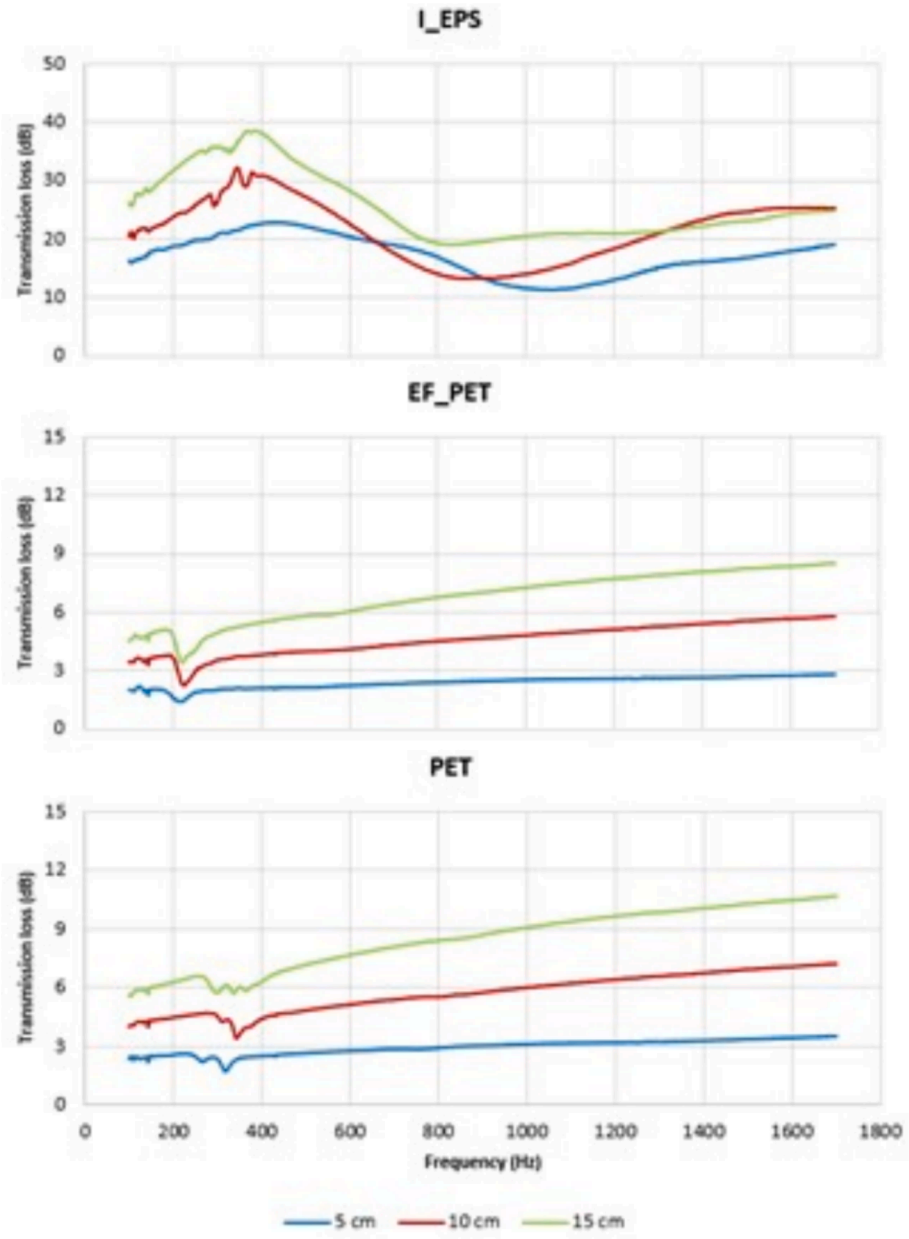

Fig. 9. Transmission loss results.

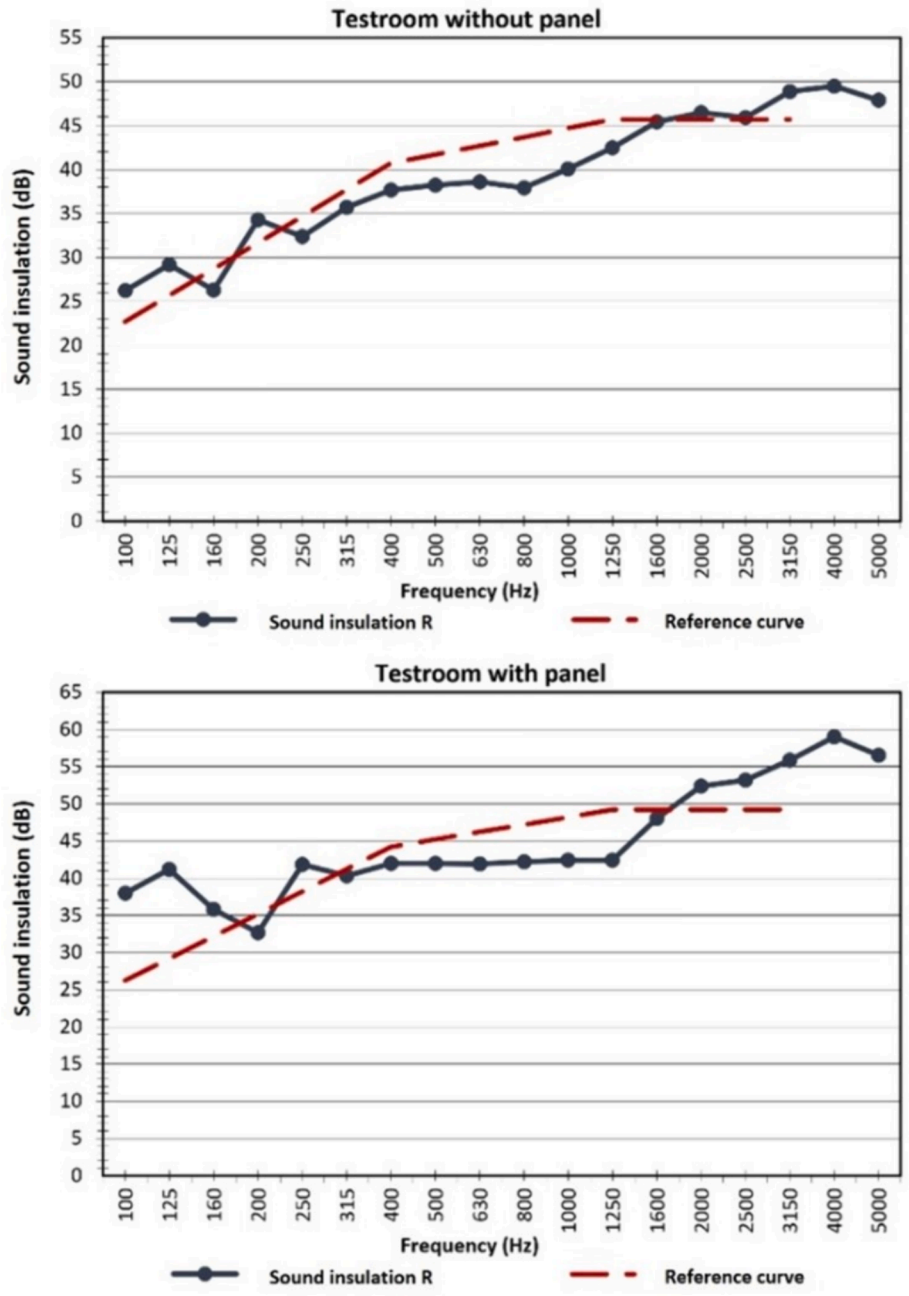

Fig. 10. Sound insulation in large-scale acoustic tests.

the lowest thermal diffusivity value of 0.81 mm^2s^{-1}. In contrast, EF_PET has the lowest volumetric specific heat value while PET and I_EPS have similar values.

4.4. Large-scale thermal analysis results

This section presents the outcomes of the thermal investigation conducted using thermo-fluxmetric analysis. The analysis encompassed three panels: MP-PET, MP-EPS, and MP-EFPET. Each panel's installation and monitoring timeline is as follows: MP-PET was placed in the test room on June 6, 2022, with thermal monitoring spanning from June 7 to June 14. Subsequently, on June 16, 2022, MP-EPS was introduced and monitored until June 20. The final panel, MP-EFPET, was installed on June 21, 2022, and monitoring occurred from June 22 to June 29. The findings for each panel are summarized in Table 5.

Given that the tests were conducted during summer, the external temperature exceeded the internal temperature of the test room. Consequently, heat flowed from the warmer outdoor environment to the cooler indoor space, resulting in a negative sign as detected by the flow sensor.

Regarding the results for thermal transmittance values, all panels demonstrate commendable insulation levels. Notably, MP-EPS presents the most promising performance, with a thermal transmittance value of 0.19 $Wm^{-2}K^{-1}$, signifying the lowest value among the panels. Following suit are MP-EFPET and MP-PET. Collectively, these findings point to I_EPS as the superior material for minimizing heat transfer within a stratigraphy. Furthermore, the congruence of these results with those derived from Hot Disk analysis lends credence to their consistency. This convergence underscores the reliability and robustness of the conclusions drawn from the thermal analysis, reinforcing the material's efficacy in reducing heat transfer.

Table 4
Hot Disk results.

	Measurement	Thermal conductivity ($Wm^{-1}K^{-1}$)	Thermal diffusivity (mm^2s^{-1})	Volumetric Specific Heat ($MJm^{-3}K^{-1}$)
PET	1	0.0432	1.2788	0.0338
	2	0.0431	1.1914	0.0361
	3	0.0427	1.2460	0.0343
	Average	**0.0430**	**1.24**	**0.035**
	St. Dev.	**0.0002**	**0.04**	**0.001**
EF_PET	1	0.0395	1.7139	0.0230
	2	0.0393	1.7917	0.0219
	3	0.0396	1.5858	0.0250
	Average	**0.0395**	**1.7**	**0.023**
	St. Dev.	**0.0002**	**0.1**	**0.002**
I_EPS	1	0.0260	0.7772	0.0335
	2	0.0263	0.8114	0.0324
	3	0.0258	0.8421	0.0306
	Average	**0.0260**	**0.81**	**0.032**
	St. Dev.	**0.0002**	**0.03**	**0.001**

4.5. Numerical investigation results

This section shows the results obtained from the validation of the prototype panel and the transmittance values obtained for the panels in real size. In particular, the first two columns of Table 6 shows the thermal transmittance values obtained in the experimental phase, i.e., in a real environment (RE), and those obtained from the validated model, i.e., virtual environment (VE). By comparing the trends of heat flow and internal and external temperature of each panel of the RE and the VE, it is possible to confirm the validation of the model given the same profile trends. Based on this validation, the thermal transmittance of the actual panels was evaluated. The last two columns in Table 6 show the thermal transmittance values evaluated with a transient study (TS) and with the additional stationary study (SS) simulated with a temperature difference of 20 °C. Again, the panel MP-EPS is found to be the best performing one, followed by MP-EFPET and MP-PET. Also in this case, these results are consistent with those obtained from small- and large-scale analyses.

Fig. 11a) shows a graphic comparison of the results obtained for the three panels in the upper part consisting of the first 35 cm without insulation. Indeed, the heat flow (red arrows) tends to pass over the top of the panel, while at the bottom the arrows are more muted, indicating a lower heat flow passage. Even in the central part of the panel shown in Fig. 11b), the influence of the insulation can be evaluated. Indeed, despite the presence of concrete that interrupts part of the insulation layer of 14 cm thick, it allows minimal heat loss. On the other hand, in the lower part of the panel shown in Fig. 11c), due to the presence of the insulation there is a reduction in heat transfer compared to the upper part. In the image for MP-EPS, the red arrows indicating heat flow are much smaller than the other two. This is consistent with all the analyses described in the previous sections, in which I_EPS insulation was always found to be the best.

In conclusion, the monitoring of the prototype panels aimed at obtaining thermal transmittance was carried out correctly. The data obtained from the numerical model for real-size panels are the most representative as they were simulated with a temperature difference between inside and outside of 20 °C. The difference obtained between the transmittances is therefore mainly due to a different geometric configuration of the panels both in terms of size and cross section and from different boundary conditions.

5. Life cycle assessment

When it comes to developing projects, it's crucial to consider the environmental implications of the chosen solution. This study is rooted in actual production data from an Italian mid-sized panel manufacturer. The company operates from two different sites: one in Bastia Umbra (PG) and the other in Aprilia (LT), both for the year 2020. The calculations were performed using SimaPro 9.3.0.2 and the ecoinvent v.3.8 database. The life cycle assessment (LCA) was carried out in compliance with recognized standards, including UNI EN ISO 14021: 2016 [62], EN ISO 14020:2001 [63], UNI EN ISO 14040:2006 [64], UNI EN ISO 14044:2021 [65], UNI EN 15804:2012+A2:2019 [66]. These standards collectively provide a comprehensive framework for evaluating the ecological ramifications of the solution, ensuring a holistic and rigorous assessment.

5.1. Goal and scope definition

This section reports the environmental impact analysis through Life Cycle Assessment (LCA) methodology. The primary goal was to scrutinize the panel's emissions across its complete life cycle, spanning from raw material sourcing for production to its ultimate disposal.

For LCA analysis, the processes considered as boundaries were selected according to the Product Category Rules (PCR) for construction materials. The cradle-to-gate approach with modules from C1 to C4 + D includes production (A1 – raw materials, A2 – transports, A3 – manufacture), end of life phase (C1 – demolition, C2 – transports, C3 – waste treatment, C4 – disposal), and recovery phase (D – potential for reuse, recovery, and recycling). Production and disassembly processes were considered under the manufacturer's direct influence and the use phase does not require water or energy.

The impact categories evaluated according to the PCR are as follows:

Table 5
Thermo-flowmetric analysis results.

	Average difference temperature	Average thermal flux	Thermal transmittance	dU
MP-PET	−6.8 °C	$-3.32\ Wm^{-2}$	$0.49\ Wm^{-2}K^{-1}$	1.99 %
MP-EPS	−7.6 °C	$-1.46\ Wm^{-2}$	$0.19\ Wm^{-2}K^{-1}$	1.41 %
MP-EFPET	−10.7 °C	$-3.86\ Wm^{-2}$	$0.36\ Wm^{-2}K^{-1}$	0.12 %

Table 6
Thermal transmittance values in RE, VE, TS, and SS.

	PANEL INSERTED IN TEST ROOM		PANEL WITH REAL DIMENSIONS	
	Thermal transmittance ($Wm^{-2}K^{-1}$) – RE	Thermal transmittance ($Wm^{-2}K^{-1}$) – VE	Thermal transmittance ($Wm^{-2}K^{-1}$) – TS	Thermal transmittance ($Wm^{-2}K^{-1}$) – SS with $\Delta T = 20$ °C
MP-PET	0.49	0.43	0.87	0.57
MP-EFPET	0.36	0.40	0.67	0.55
MP-EPS	0.19	0.18	0.41	0.45

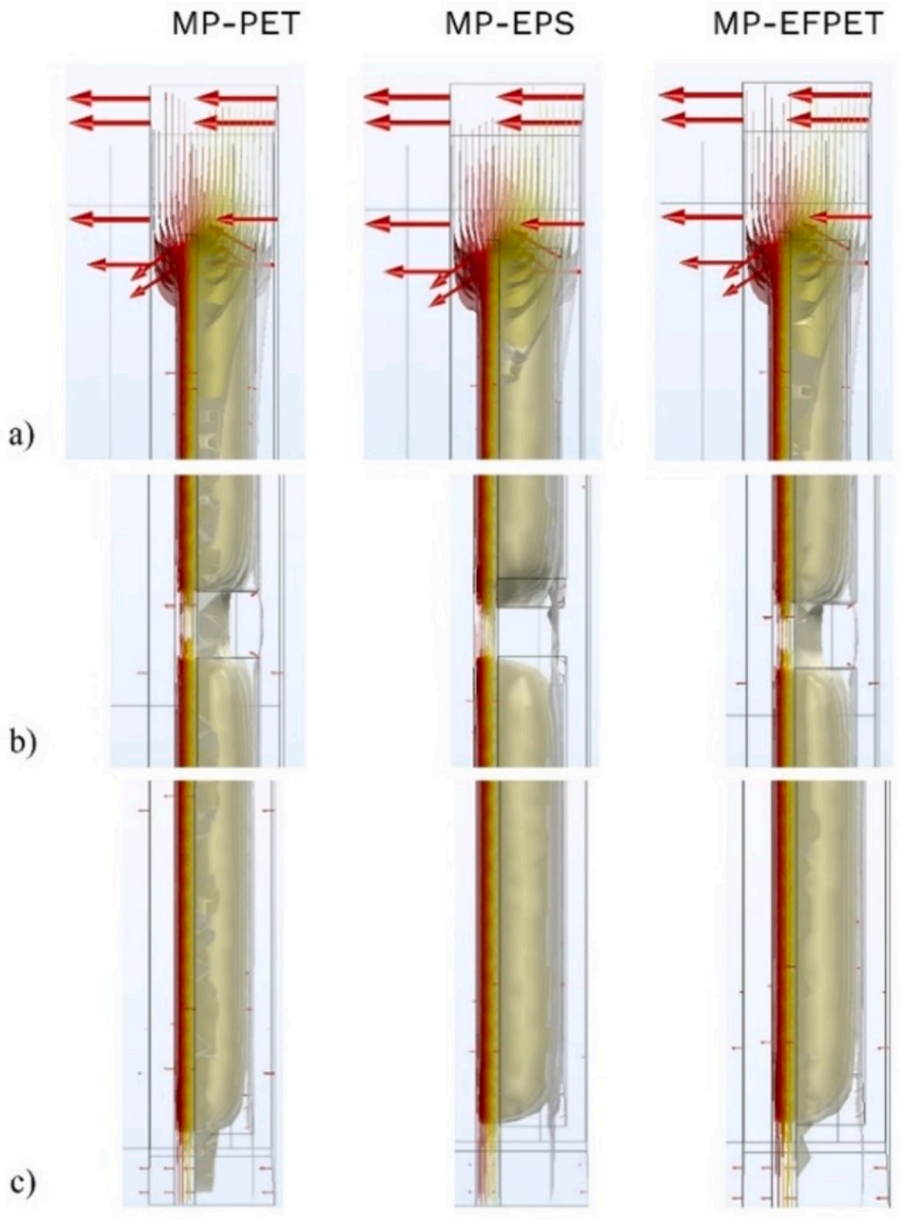

Fig. 11. Heat flow trend.

climate change (GWP – total), ozone depletion (ODP), photochemical ozone formation (POCP), acidification (AP), eutrophication – freshwater (EP – freshwater), eutrophication – marine (EP – marine), eutrophication – terrestrial (EP – terrestrial), water use (WDP), resource use – fossils (ADP fossil), resource use – minerals and metals (ADP minerals & metals), climate change – fossil (GWP – fossil), climate change – biogenic (GWP – biogenic), climate change – land use, and LU change (GWP – luluc).

5.1.1. Study object description

Two types of pre-stressed reinforced concrete panels filled with recycled polyester fibers were investigated. At least 85 % of the insulation comes from recycled plastic bottles (PET), which implies that the impacts for the raw materials were not considered according to the polluters pay criteria. This analysis studies the panel in 20 cm (TH20) and 30 cm (TH30) thickness realized in the Bastia Umbra (B) and Aprilia (A) sites. Specifically, Table 7 highlights the main components in percentages of these panels.

Table 7
Main panel components percentage.

	TH20 – B	TH30 – B	TH20 – A	TH30 – A
Steel	2.91 %	3.45 %	3.64 %	4.82 %
Dismantling oil	0.04 %	0.03 %	0.04 %	0.03 %
Cement	91.56 %	90.26 %	94.93 %	93.40 %
Filler	4.51 %	4.37 %	–	–
Fluidifier	0.22 %	0.21 %	0.14 %	0.14 %
PET	0.76 %	1.68 %	0.99 %	1.36 %
Accelerator	–	–	0.26 %	0.26 %
Total	100 %	100 %	100 %	100 %

5.1.2. Declared unit and allocation criteria

The declared unit corresponds to the material and energy flows required to produce 1 m^2 of each type of panel TH20-B, TH20-A, TH30-B, and TH30-A and the processes selected correspond to Cut-off, Unit model.

The allocation of inputs and outputs were based on the m^3 and m^2

produced in the two sites for each model analyzed, according to the formula:

$$Allocation = \left[\left(Data_{product} \times m^3_{pannTHx}/m^3_{tot}\right)\right] \times \left[\left(1/m^3_{tot}\right)\right]$$

5.2. Life cycle inventory

The production phase includes modules A1, A2 and A3. Module A1 refers to the supply of raw materials needed to produce the panel, i.e., steel, electrowelded mesh, dismantling oil, cement, gravel, sand, water, filler, fluidifier, PET, and accelerator. In detail, steel was considered with 100 %, 98 %, 97 % and ND (0 %) recycled amount. Specifically, the inputs are the same between the two sites, except for filler and accelerant, used at B and A respectively. Technical data was sourced from the material data sheets: fluidifier has a density of 1.06 g/ml, the accelerant of 1.1 g/ml and the disarming oil of 0.86 g/cc. The total raw materials processed to produce 1 m^2 of panel in B for the 20 cm thick panel is 344.5 kg and 381.9 kg for the 30 cm thick panel. In A, the total quantity is 315.9 kg for the 20 cm thick panel and 420.5 kg for the 30 cm thick panel.

Module A2 includes transportation of the supply materials used for the panels production. Using kgkm as the unit of measurement, distances between the supplying companies were then multiplied by the purchased quantity of each material required to produce 1 m^2 of panel. The transport considered for the routes is an articulated lorry.

In module A3 are included the energy consumption with local market energy mix selected (medium voltage) and fuel for in-site transportation, the atmospheric emissions (particulates), and the waste treatment to produce panels.

The end-of-life phase corresponds to modules C1 to C4. In C1, the panel demolition scenario is modelled considering 2.5 l of diesel (0.835 kg/l density [67]) consumption by a demolition machine per m^3 of panel. This estimation was obtained from a previous study conducted by the producer. The fuel needed per m^3 was divided by the area of panels produced at each production site.

Module C2 considers the transportation to a hypothetical recipient company to which materials from demolition of each site is to be sent. A distance of 20 km is assumed for both sites and the transportation mean is a lorry [68].

Module C3 examines the treatment of waste obtained from demolition services. Waste is processed according to percentages indicated in the literature [68] for construction and demolition. Therefore, recycling reaches 100 % for concrete, 89.3 % for steel, and 36.4 % for plastic polyethylene terephthalate (PET).

Module C4 deals with the processing of materials demolished that were not treated in the previous module according literature [69]: remaining waste materials is destined partly to landfill (51.1 %) and partly to incineration (48.9 %).

On the other hand, the recovery phase considers module D, which represents an assumed scenario of possible benefits of net flows in the end-of-life phase. In this case, recycled items were used as substitutes for raw materials for new products. Thus, impacts for production were considered as avoided.

5.3. Results and discussion

After entering the inputs explained in the previous section, presented in detail in the Annex, impacts were characterized using the EN 15804+A2 method as stablished by the PCR. Table 8 shows the total impact given by the panels for each of the 13 impact categories listed in Section 5.1.

Module A1 was accessed separately as it contributes to more than 80 % in GWP to the impact in all models. Furthermore, comparing the production of the 20-cm-thick panel from site B and A, in terms of climate change, the panel from A impacts 3 % less than the one from B, while the 30-cm-thick panel made at A impacts 11 % more than the same one made at B. Indeed, for the 20 cm panel, the quantities of gravel, sand, water, and fluidifier used for A are lower. On the other hand, for the 30 cm panel, the quantities of recycled steel, electrowelded mesh, disarming oil, cement, gravel, sand, and water are greater for the A site than for the B site. This therefore justifies the resulting impacts of A1 for the panels.

Table 8
Total emissions results for the four panels analyzed.

	Unit	TH20 – B	TH30 – B	TH20 – A	TH30 – A
GWP – total	kg CO2 eq	7.62E + 01	9.44E + 01	7.93E + 01	1.09E + 02
ODP	kg CFC11 eq	1.11E-05	2.07E-05	1.25E-05	2.05E-05
POCP	kg NMVOC eq	2.61E-01	3.38E-01	2.68E-01	3.86E-01
AP	mol H + eq	3.08E-01	3.76E-01	2.99E-01	4.24E-01
EP – freshwater	kg P eq	1.50E-03	1.92E-03	1.55E-03	2.32E-03
EP – marine	kg N eq	7.83E-02	9.51E-02	8.04E-02	1.12E-01
EP – terrestrial	mol N eq	8.64E-01	1.05E + 00	8.92E-01	1.25E + 00
WDP	m3 depriv.	1.99E + 01	2.43E + 01	1.77E + 01	2.66E + 01
ADP fossil	MJ	6.52E + 02	8.40E + 02	6.59E + 02	9.64E + 02
ADP minerals & metals	kg Sb eq	3.15E-04	5.67E-04	4.48E-04	7.18E-04
GWP – fossil	kg CO2 eq	7.41E + 01	9.16E + 01	7.71E + 01	1.06E + 02
GWP – biogenic	kg CO2 eq	1.47E + 00	2.35E + 00	1.57E + 00	2.47E + 00
GWP – luluc	kg CO2 eq	5.21E-01	4.70E-01	5.15E-01	5.50E-01

Fig. 12.a shows the impacts of the various modules in terms of kg CO_2 eq, which is the representative and most important category for expressing the impact on global warming. To analyze the impacts of this phase in more detail, each component in A1 was analyzed in terms of kg CO2 eq emitted for each kg of material considered to understand which material has the greatest impact (Fig. 12.b).

The analysis showed that, individually, the most harmful material is the dismantling oil, with 3.86 kg CO2 eq emitted for each kg of product. Given the small quantity used in the production (Fig. 13.a), the emission of this product corresponds to less than 1 % of the total emissions for each 1 m^2 of panel. On the other hand, cement with an emission comparable to 0.8 kg CO2 eq per kg and corresponding to 15–17 % of total panel weight, cement accounts for about 50–60 % of the final emissions per m^2 of panel (Fig. 13.b).

5.4. Sensitivity analysis

Considering the contribution of cement, sensitivity analysis was performed proposing an alternative material changing the input from "Cement, alternative constituents 6–20 % {Europe without Switzerland}| production| Cut-off, U" to "Cement, limestone 6–20 % {RoW}| cement production | Cut-off, U" from the ecoinvent v.3.8 database.

Results obtained from limestone cement, with emission of 0.74 kg CO_2 eq per kg, corresponds to approximately 6.8 % less in comparison to the previous cement. Therefore, the substitution of this material could lead to a reduction in emissions of about 4 % per m^2 of panel.

6. Discussion and conclusions

The following work proposes a multi-objective, multi-scale and

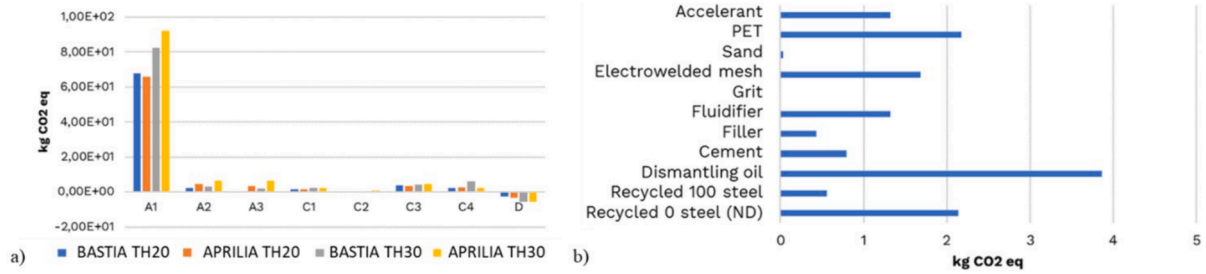

Fig. 12. a) Indicators of climate change factors in production sites for each stage, b) Material emissions for kg of each product.

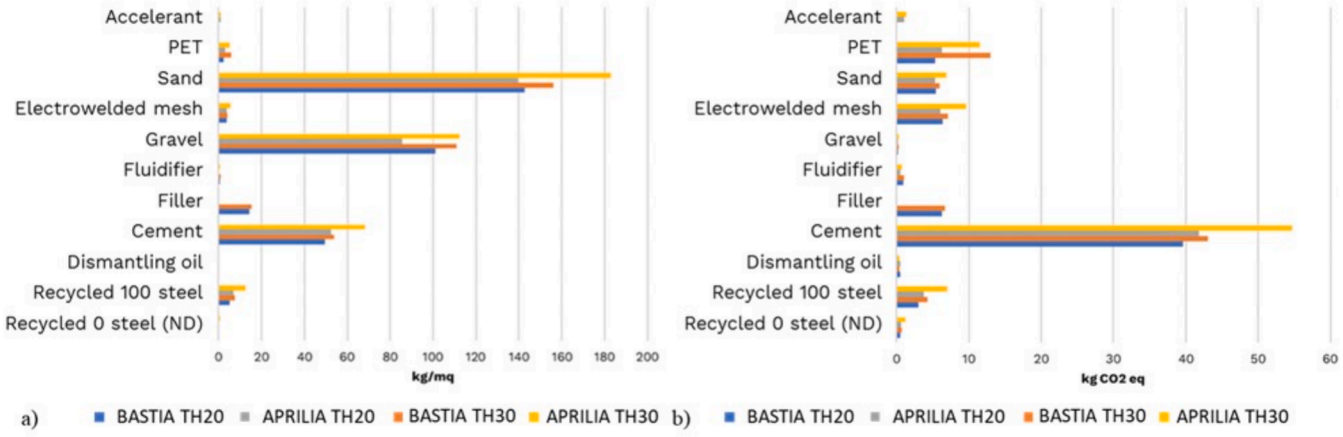

Fig. 13. a) Materials used to produce 1 m^2 of panel, b) Emissions in kg CO2 eq for each material.

multi-approach analysis on innovative panels made of components derived from recycled materials. Indeed, in this work selected materials were chosen to produce a new efficient, sustainable, and functional prefabricated panel.

In particular, small-scale sound insulation tests were conducted on three types of insulation produced from waste materials: two derived from plastic fibers (PET and EF_PET) and one graphite-added EPS (I_EPS). From the results obtained, it was assessed that the two plastic-derived insulators perform less well than the I_EPS insulation, probably due to the material structure. Sound insulation tests were also conducted on a large scale in test rooms by installing precast concrete panels with the interposition of the three types of insulation (MP-PET, MP-EFPET, MP-EPS). Their performance was evaluated by comparing the facade sound insulation rating index of the test room with and without the panel, obtaining promising results with an increase in sound insulation that highlights their potential.

Small-scale thermal tests showed that all insulation materials tested (I_EPS, PET and EF_PET) have good insulation properties, i.e., always below 0.065 $Wm^{-1}K^{-1}$. These properties were also confirmed by the large-scale thermal analyses involving the installation of the 3 precast concrete panels in test room. Indeed, the thermal transmittance results were consistent with the values obtained from the small-scale thermal tests, confirming I_EPS as the best insulator, followed by EF_PET and PET. Moreover, based on this thermal monitoring, a numerical analysis was carried out to assess the transmittance of the panel with real sections and dimensions, reporting results consistent with those obtained from the other analyses.

In addition to material testing, the life cycle of panel production with PET was analyzed in terms of environmental impact, following a "cradle-to-gate" approach. The study found that concrete contributes the greatest impact, no doubt due to the significant total weight on the panel. However, replacing the type of concrete could lead to lower impacts, improving the performance of this new system.

The investigated panel comprises a concrete slab-insulation layer-concrete slab configuration, which allows the use of various types of materials available for the insulation layer, further improving its sustainability. In this context, the use of wood-wool-cement composite panels (WWCP) for precast walls can improve sustainability by offering environmental benefits and structural integrity [70]. Furthermore, the construction of prefabricated timber structures is also a sustainable option, promoting environmental merits and market competitiveness [71], as well as modular construction systems with solid wood panels also further emphasise sustainability by emphasising renewable and recyclable resources [44].

In the pursuit of sustainability, selecting eco-friendly materials for the insulation layer is also crucial. Innovative solutions, such as biomass-based composite materials derived from sawdust and geopolymers, provide effective insulation while minimizing environmental impact, contributing to greener construction practices [72]. The realm of prefabricated systems offers diverse approaches and technologies to enhance sustainability, ranging from material selection to composition considerations, enabling optimization of environmental impact. It should be noted that the performance of precast panels varies with design, emphasizing the importance of understanding their properties and selecting the most suitable option based on climatic conditions.

Furthermore, during the manufacturing and installation of prefabricated panels, various factors can impact their performance, including construction and installation methods. Practical elements may influence performance, leading to issues like water absorption, rising damp, or thermal bridging. Introducing moisture barriers into panels can address these challenges by incorporating layers or treatments that act as robust barriers against water and moisture migration. Options include waterproof coatings or materials resistant to moisture infiltration. Therefore, attention to design and installation processes is vital to mitigate thermal bridging risks, possibly through specific construction details, thermal breaks, or additional insulation at critical points.

Implementing regular monitoring and maintenance protocols is crucial, involving routine inspections for timely issue identification and necessary repairs or component replacements. Exploring innovative materials with enhanced properties, such as high-performance insulation or advanced coatings, offers further avenues. For example, aerogels, known for their lightweight and insulating properties, can significantly enhance thermal efficiency and comfort in buildings. Incorporating aerogel sheets into prefabricated panels can reduce heat transfer and mitigate thermal bridging, while their moisture resistance is beneficial in challenging environmental conditions. Moreover, prefabricated panels offer significant cost advantages in building construction. Their efficient production processes reduce labor and site management costs, while minimizing material waste enhances resource utilization and lowers production costs. Furthermore, their superior thermal and acoustic properties contribute to long-term cost savings by reducing reliance on heating and cooling systems.

In conclusion, the innovative proposal of this prefabricated panel seems to be technically and environmentally promising and, although this study focused on the Mediterranean climate of Perugia, its methodology remains solid and applicable to different urban contexts with the understanding that considering meteorological, spatial and geomorphological factors is fundamental to ensure the methodology's relevance in different geographical contexts. For material selection, insulators derived from plastic have good properties, but not at the level of I_EPS. Therefore, it could be considered to improve the production of such insulators by achieving higher thermal and acoustic properties. Substituting cement type could contribute to further reducing the environmental impact. This study could then be implemented by selecting several promising recycled materials to be included in the production cycle of prefabricated panels, as today's goal is to reduce environmental pollution and make efficient buildings.

CRediT authorship contribution statement

Silvia Cavagnoli: Writing – original draft, Visualization, Methodology, Investigation, Formal analysis, Data curation. **Claudia Fabiani:** Writing – review & editing, Validation, Supervision, Methodology, Investigation, Data curation, Conceptualization. **Fabiana Frota de Albuquerque Landi:** Writing – review & editing, Formal analysis, Data curation. **Anna Laura Pisello:** Writing – review & editing, Supervision, Resources, Project administration, Methodology, Investigation, Funding acquisition, Conceptualization.

Declaration of competing interest

The authors declare that they have no known competing financial interests or personal relationships that could have appeared to influence the work reported in this paper.

Data availability

Data will be made available on request.

Acknowledgments

S.C. and F.L.'s acknowledgements are due to the PhD school in Energy and Sustainable Development, University of Perugia, Italy. All authors thank Manini Prefabbricati S.p.A. for supplying and installing the materials and prefabricated panels and supporting the R&D project. This work was partly funded by the Italian Ministry of Research through the THE-UNKNOWN (ProtP2022NM5L7) "equivalent THErmo-physical properties for UNKNOWN composition of building walls" project, and the LIGNOCAP (Prot2022M8EEFF) "Bio-based insulation panels in building envelope and cooling systems for improving acoustic and thermal comfort and mitigating urban heat islands" project, within the PRIN 2022 program, as well as the Fondazione Cassa di Risparmio di Perugia through the project "LONG-LIFE - Innovative technoLOgies for enhanciNG LIFE-cycle sustainability of reinforced concrete structures" project (Project Code: 21071 (2022.0400). The authors also thank RSE S.p.A. for supporting the dissemination of this and other initiatives by EAPLAB.

Annex

PRODUCTS	Input	Unit
Accelerant	1	kg
Materials/fuels		
Plasticiser, for concrete, based on sulfonated melamine formaldehyde {GLO}| plasticiser production, for concrete, based on sulfonated melamine formaldehyde | Cut-off, U	1	kg
Electricity/heat		
Transport, freight, lorry 16-32 metric ton, EURO4 {RER}| market for	597	kgkm
Products		
Recycled 0 steel (ND) Aprilia	1	kg
Materials/fuels		
raw_materials_Steel, low-alloyed {RER}| steel production, converter, low-alloyed | Cut-off, U	1	kg
Electricity/heat		
Transport, freight, lorry 16-32 metric ton, EURO4 {RER}| market for	586	kgkm
Products		
Recycled 0 steel (ND) Bastia Umbra	1	kg
Materials/fuels		
raw_materials_Steel, low-alloyed {RER}| steel production, converter, low-alloyed | Cut-off, U	1	kg
Electricity/heat		
Transport, freight, lorry 16-32 metric ton, EURO4 {RER}| market for	420	kgkm
Products		
100% recycled steel Aprilia	1	kg
Materials/fuels		
Steel, low-alloyed {EU without Switzerland and Austria}| steel production, electric, low-alloyed | Cut-off, U – 100%	1	kg
Electricity/heat		
Transport, freight, lorry 16-32 metric ton, EURO4 {RER}| market for	411.79	kgkm
Products		
100% recycled steel Bastia Umbra	1	kg
Materials/fuels		

(*continued on next page*)

(*continued*)

PRODUCTS	Input	Unit
100_Steel, low-alloyed {EU without Switzerland and Austria}| steel production, electric, low-alloyed | Cut-off, U – 100%	1	kg
Electricity/heat		
Transport, freight, lorry 16-32 metric ton, EURO4 {RER}| market for	492.14	kgkm
Products		
Water	1	kg
Materials/fuels		
Tap water {EU without Switzerland}| market for tap water | Cut-off, U	1	kg
Products		
Dismantling oil Aprilia	1	kg
Materials/fuels		
Alkyd resin, long oil, without solvent, in 70% white spirit solution state {RER}| alkyd resin production, long oil, product in 70% white spirit solution state | Cut-off, U	1	kg
Electricity/heat		
Transport, freight, lorry 16-32 metric ton, EURO4 {RER}| market for	39	kgkm
Products		
Dismantling oil Bastia Umbra	1	kg
Materials/fuels		
Alkyd resin, long oil, without solvent, in 70% white spirit solution state {RER}| alkyd resin production, long oil, product in 70% white spirit solution state | Cut-off, U	1	kg
Electricity/heat		
Transport, freight, lorry 16-32 metric ton, EURO4 {RER}| market for	250	kgkm
System description		
Products		
cement 42,5 R II A Aprilia	1	kg
Materials/fuels		
Cement, CEM II/A {EU without Switzerland}| cement production, CEM II/A | Cut-off, U	1	kg
Electricity/heat		
Transport, freight, lorry 16-32 metric ton, EURO4 {RER}| market for	154	kgkm
Products		
cement 42,5 R II A Bastia Umbra	1	kg
Materials/fuels		
Cement, CEM II/A {EU without Switzerland}| cement production, CEM II/A | Cut-off, U	1	kg
Electricity/heat		
Transport, freight, lorry 16-32 metric ton, EURO4 {RER}| market for	56	kgkm
Products		
cement 42,5 R II A_module_C3	1	kg
Materials/fuels		
Cement, CEM II/A {EU without Switzerland}| cement production, CEM II/A | Cut-off, U	0	kg
Electricity/heat		
Transport, freight, lorry 16-32 metric ton, EURO4 {RER}| market for	0	kgkm
Final waste flows		
Waste to treatment		
Waste cement in concrete and mortar {EU without Switzerland}| treatment of waste cement in concrete and mortar, collection for final disposal | Cut-off, U	1	kg
Products		
cement 42,5 R II A_module_C4	1	kg
Materials/fuels		
Cement, CEM II/A {EU without Switzerland}| cement production, CEM II/A | Cut-off, U	0	kg
Electricity/heat		
Transport, freight, lorry 16-32 metric ton, EURO4 {RER}| market for	0	kgkm
Final waste flows		
Waste to treatment		
Waste concrete {EU without Switzerland}| treatment of waste concrete, inert material landfill | Cut-off, U	0	kg
Waste cement-fibre slab, dismantled {RoW}| treatment of waste cement-fibre slab, municipal incineration | Cut-off, U	0	kg
Products		
cement_SENS	1	kg
Materials/fuels		
Cement, CEM II/A {EU without Switzerland}| cement production, CEM II/A | Cut-off, U	1	kg
Cement, limestone 6-20% {RoW}| cement production, limestone 6-20% | Cut-off, U	1	kg
Products		
Filler Aprilia	1	kg
Materials/fuels		
Acrylic filler {RER}| acrylic filler production | Cut-off, U	1	kg
Electricity/heat		
Transport, freight, lorry 16-32 metric ton, EURO4 {RER}| market for	114	kgkm
Products		
Filler Bastia Umbra	1	kg
Materials/fuels		
Acrylic filler {RER}| acrylic filler production | Cut-off, U	1	kg
Electricity/heat		
Transport, freight, lorry 16-32 metric ton, EURO4 {RER}| market for	55	kgkm
System description		
Products		
Fluidifier Aprilia	1	kg
Materials/fuels		

(*continued on next page*)

(*continued*)

PRODUCTS	Input	Unit
Plasticiser, for concrete, based on sulfonated melamine formaldehyde {GLO}| plasticiser production, for concrete, based on sulfonated melamine formaldehyde | Cut-off, U	1	kg
Electricity/heat		
Transport, freight, lorry 16-32 metric ton, EURO4 {RER}| market for	597	kgkm
Products		
Fluidifier Bastia Umbra	1	kg
Materials/fuels		
Plasticiser, for concrete, based on sulfonated melamine formaldehyde {GLO}| plasticiser production, for concrete, based on sulfonated melamine formaldehyde | Cut-off, U	1	kg
Electricity/heat		
Transport, freight, lorry 16-32 metric ton, EURO4 {RER}| market for	420	kgkm
Products		
Gravel Aprilia	1	kg
Materials/fuels		
Gravel, round {CH}| gravel and sand quarry operation | Cut-off, U	1	kg
Electricity/heat		
Transport, freight, lorry 16-32 metric ton, EURO4 {RER}| market for	50.34	kgkm
Products		
Gravel Bastia Umbra	1	kg
Materials/fuels		
Gravel, round {CH}| gravel and sand quarry operation | Cut-off, U	1	kg
Electricity/heat		
Transport, freight, lorry 16-32 metric ton, EURO4 {RER}| market for	22.4	kgkm
Products		
Panel_TH20_Aprilia	**1**	**m2**
Materials/fuels		
TH20_Aprilia	**1**	**m2**
Electricity/heat		
Electricity, medium voltage {IT}| market for electricity, medium voltage | Cut-off, U	7.51	kWh
Electricity, low voltage {IT}| electricity production, photovoltaic, 570kWp open ground installation, multi-Si | Cut-off, U	10.67	kWh
Electricity, medium voltage {IT}| market for electricity, medium voltage | Cut-off, U	-5.42	kWh
Diesel {EU without Switzerland}| market for diesel | Cut-off, U	0.054*0.844	kg
Transport, freight, lorry 3.5-7.5 metric ton, EURO4 {RER}| market for	1316.96	kgkm
Heat, central or small-scale, natural gas {EU without Switzerland}| heat production, natural gas, at boiler atmospheric non-modulating <100kW | Cut-off, U – just combustion	0.228	kWh
Natural gas, high pressure {IT}| market for natural gas, high pressure | Cut-off, U	0.025	m3
Diesel, burned in building machine {GLO}| processing | Cut-off, U	42.8*0.0456	MJ
Particulates, < 10 um	0.312	mg
Hazardous waste, for incineration {EU without Switzerland}| treatment of hazardous waste, hazardous waste incineration | Cut-off, U	0.034	kg
Scrap steel {EU without Switzerland}| treatment of scrap steel, inert material landfill | Cut-off, U	2.26	kg
Waste bitumen {EU without Switzerland}| treatment of waste bitumen, sanitary landfill | Cut-off, U	0.25	kg
Waste cement, hydrated {EU without Switzerland}| treatment of waste cement, hydrated, residual material landfill | Cut-off, U	25.15	kg
Inert waste, for final disposal {RoW}| treatment of inert waste, inert material landfill | Cut-off, U	0.11	kg
Waste wood, untreated {RoW}| treatment of waste wood, untreated, municipal incineration | Cut-off, U	0.22	kg
Waste polyethylene {IT}| market for waste polyethylene | Cut-off, U – no transport	0	kg
Waste plastic, mixture {IT}| market for waste plastic, mixture | Cut-off, U – no transport	0.04+0.01	kg
Waste electric and electronic equipment {GLO}| treatment of waste electric and electronic equipment, shredding | Cut-off, U	0.01	kg
Products		
Panel_TH20_Bastia Umbra	**1**	**m2**
Materials/fuels		
TH20_Bastia Umbra	**1**	**m2**
Electricity/heat		
Electricity, medium voltage {IT}| market for electricity, medium voltage | Cut-off, U	4.49	kWh
Electricity, low voltage {IT}| electricity production, photovoltaic, 570kWp open ground installation, multi-Si | Cut-off, U	3.86	kWh
Electricity, medium voltage {IT}| market for electricity, medium voltage | Cut-off, U	-1.35	kWh
Diesel {EU without Switzerland}| market for diesel | Cut-off, U	0.063*0.844	kg
Transport, freight, lorry 3.5-7.5 metric ton, EURO4 {RER}| market for	1746.42	kgkm
Heat, central or small-scale, natural gas {EU without Switzerland}| heat production, natural gas, at boiler atmospheric non-modulating <100kW | Cut-off, U – just combustion	2.75	kWh
Natural gas, high pressure {IT}| market for natural gas, high pressure | Cut-off, U	0.307	m3
Diesel, burned in building machine {GLO}| processing | Cut-off, U	42.8*0.0532	MJ
Particulates, < 10 um	1.61	mg
Waste to treatment	0.005	kg
Hazardous waste, for incineration {EU without Switzerland}| treatment of hazardous waste, hazardous waste incineration | Cut-off, U		
Scrap steel {EU without Switzerland}| treatment of scrap steel, inert material landfill | Cut-off, U	3.64	kg
Waste bitumen {EU without Switzerland}| treatment of waste bitumen, sanitary landfill | Cut-off, U	0.14	kg
Waste cement, hydrated {EU without Switzerland}| treatment of waste cement, hydrated, residual material landfill | Cut-off, U	47.52	kg
Inert waste, for final disposal {RoW}| treatment of inert waste, inert material landfill | Cut-off, U	0.34	kg
Waste wood, untreated {RoW}| treatment of waste wood, untreated, municipal incineration | Cut-off, U	0.18	kg
Waste polyethylene {IT}| market for waste polyethylene | Cut-off, U – no transport	0.02	kg
Products		
Panel_TH30_Aprilia	**1**	**m2**
Materials/fuels		
TH30_Aprilia	**1**	**m2**
Electricity/heat		
Electricity, medium voltage {IT}| market for electricity, medium voltage | Cut-off, U	11.27	kWh

(*continued on next page*)

(*continued*)

PRODUCTS	Input	Unit
Electricity, low voltage {IT}| electricity production, photovoltaic, 570kWp open ground installation, multi-Si | Cut-off, U	16.01	kWh
Electricity, medium voltage {IT}| market for electricity, medium voltage | Cut-off, U	-8.13	kWh
Diesel {EU without Switzerland}| market for diesel | Cut-off, U	0.081*0.844	kg
Transport, freight, lorry 3.5-7.5 metric ton, EURO4 {RER}| market for	1975.4	kgkm
Heat, central or small-scale, natural gas {EU without Switzerland}| heat production, natural gas, at boiler atmospheric non-modulating <100kW | Cut-off, U – just combustion	0.342	kWh
Natural gas, high pressure {IT}| market for natural gas, high pressure | Cut-off, U	0.038	m3
Diesel, burned in building machine {GLO}| processing | Cut-off, U	42.8*0.0684	MJ
Particulates, < 10 um	0.47	mg
Final waste flows		
Waste to treatment		
Hazardous waste, for incineration {EU without Switzerland}| treatment of hazardous waste, hazardous waste incineration | Cut-off, U	0.051	kg
Scrap steel {EU without Switzerland}| treatment of scrap steel, inert material landfill | Cut-off, U	3.39	kg
Waste bitumen {EU without Switzerland}| treatment of waste bitumen, sanitary landfill | Cut-off, U	0.38	kg
Waste cement, hydrated {EU without Switzerland}| treatment of waste cement, hydrated, residual material landfill | Cut-off, U	37.73	kg
Inert waste, for final disposal {RoW}| treatment of inert waste, inert material landfill | Cut-off, U	0.17	kg
Waste wood, untreated {RoW}| treatment of waste wood, untreated, municipal incineration | Cut-off, U	0.32	kg
Waste polyethylene {IT}| market for waste polyethylene | Cut-off, U – no trasport	0	kg
Waste plastic, mixture {IT}| market for waste plastic, mixture | Cut-off, U – no trasport	0.06+0.01	kg
Waste electric and electronic equipment {GLO}| treatment of waste electric and electronic equipment, shredding | Cut-off, U	0.02	kg
Products		
Panel_TH30_Bastia Umbra	**1**	**m2**
Materials/fuels		
TH30_Bastia Umbra	**1**	**m2**
Electricity/heat		
Electricity, medium voltage {IT}| market for electricity, medium voltage | Cut-off, U	6.74	kWh
Electricity, low voltage {IT}| electricity production, photovoltaic, 570kWp open ground installation, multi-Si | Cut-off, U	5.79	kWh
Electricity, medium voltage {IT}| market for electricity, medium voltage | Cut-off, U	-2.02	kWh
Diesel {EU without Switzerland}| market for diesel | Cut-off, U	0.095*0.844	kg
Transport, freight, lorry 3.5-7.5 metric ton, EURO4 {RER}| market for	2619.47	kgkm
Heat, central or small-scale, natural gas {EU without Switzerland}| heat production, natural gas, at boiler atmospheric non-modulating <100kW | Cut-off, U – just combustion	4.12	kWh
Natural gas, high pressure {IT}| market for natural gas, high pressure | Cut-off, U	0.461	m3
Diesel, burned in building machine {GLO}| processing | Cut-off, U	42.8*0.0802	MJ
Particulates, < 10 um	2.42	mg
Final waste flows		
Waste to treatment		
Hazardous waste, for incineration {EU without Switzerland}| treatment of hazardous waste, hazardous waste incineration | Cut-off, U	0.008	kg
Scrap steel {EU without Switzerland}| treatment of scrap steel, inert material landfill | Cut-off, U	5.47	kg
Waste bitumen {EU without Switzerland}| treatment of waste bitumen, sanitary landfill | Cut-off, U	0.21	kg
Waste cement, hydrated {EU without Switzerland}| treatment of waste cement, hydrated, residual material landfill | Cut-off, U	71.27	kg
Inert waste, for final disposal {RoW}| treatment of inert waste, inert material landfill | Cut-off, U	0.51	kg
Waste wood, untreated {RoW}| treatment of waste wood, untreated, municipal incineration | Cut-off, U	0.27	kg
Waste polyethylene {IT}| market for waste polyethylene | Cut-off, U – no transport	0.03	kg
Products		
Electrowelded mesh Aprilia	1	kg
Materials/fuels		
Reinforcing steel {EU without Austria}| reinforcing steel production | Cut-off, U – 97%	1	kg
Electricity/heat		
Transport, freight, lorry 16-32 metric ton, EURO4 {RER}| market for	570	kgkm
Products		
Electrowelded mesh Bastia Umbra	1	kg
Materials/fuels		
Reinforcing steel {EU without Austria}| reinforcing steel production | Cut-off, U – 97%	1	kg
Electricity/heat		
Transport, freight, lorry 16-32 metric ton, EURO4 {RER}| market for	380	kgkm
Products		
Electrowelded mesh_module_C3	1	kg
Materials/fuels		
Reinforcing steel {EU without Austria}| reinforcing steel production | Cut-off, U – 97%	0	kg
Electricity/heat		
Transport, freight, lorry 16-32 metric ton, EURO4 {RER}| market for	0	kgkm
Final waste flows		
Waste to treatment		
Steel and iron (waste treatment) {GLO}| recycling of steel and iron | Cut-off, U	0.893	kg
Products		
Electrowelded mesh_module_C4	1	kg
Materials/fuels		
Reinforcing steel {EU without Austria}| reinforcing steel production | Cut-off, U – 97%	0	kg
Electricity/heat		
Transport, freight, lorry 16-32 metric ton, EURO4 {RER}| market for	0	kgkm
Final waste flows		
Waste to treatment		
Scrap steel {EU without Switzerland}| treatment of scrap steel, inert material landfill | Cut-off, U	0.055	kg
Steel in car shredder residue {RoW}| treatment of steel in car shredder residue, municipal incineration | Cut-off, U	0.052	kg
Products		

(*continued on next page*)

(*continued*)

PRODUCTS	Input	Unit
Sand Aprilia	1	kg
Materials/fuels		
Silica sand {RoW}| silica sand production | Cut-off, U	1	kg
Electricity/heat		
Transport, freight, lorry 16-32 metric ton, EURO4 {RER}| market for	57	kgkm
Products		
Sand Bastia Umbra	1	kg
Materials/fuels		
Silica sand {RoW}| silica sand production | Cut-off, U	1	kg
Electricity/heat		
Transport, freight, lorry 16-32 metric ton, EURO4 {RER}| market for	26.7	kgkm
Products		
PET Aprilia	1	kg
Materials/fuels		
Polyethylene terephthalate, granulate, amorphous, recycled {EU without Switzerland}| polyethylene terephthalate production, granulate, amorphous, recycled | Cut-off, U	0.75	kg
Polyethylene terephthalate, granulate, bottle grade {RER}| polyethylene terephthalate production, granulate, bottle grade | Cut-off, U	0.25	kg
Electricity/heat		
Polymer foaming {RER}| polymer foaming | Cut-off, U	1	kg
Transport, freight, lorry 16-32 metric ton, EURO4 {RER}| market for	347	kgkm
Products		
PET Bastia Umbra	1	kg
Materials/fuels		
Polyethylene terephthalate, granulate, amorphous, recycled {EU without Switzerland}| polyethylene terephthalate production, granulate, amorphous, recycled | Cut-off, U	0.75	kg
Polyethylene terephthalate, granulate, bottle grade {RER}| polyethylene terephthalate production, granulate, bottle grade | Cut-off, U	0.25	kg
Electricity/heat		
Polymer foaming {RER}| polymer foaming | Cut-off, U	1	kg
Transport, freight, lorry 16-32 metric ton, EURO4 {RER}| market for	184	kgkm
Products		
PET_module_C3	1	kg
Materials/fuels		
Polyethylene terephthalate, granulate, amorphous, recycled {EU without Switzerland}| polyethylene terephthalate production, granulate, amorphous, recycled | Cut-off, U	0	kg
Polyethylene terephthalate, granulate, bottle grade {RER}| polyethylene terephthalate production, granulate, bottle grade | Cut-off, U	0	kg
Electricity/heat		
Polymer foaming {RER}| polymer foaming | Cut-off, U	0	kg
Transport, freight, lorry 16-32 metric ton, EURO4 {RER}| market for	0	kgkm
Final waste flows		
Waste to treatment		
PET (waste treatment) {GLO}| recycling of PET | Cut-off, U	0.364	kg
System description		
Products		
PET_module_C4	1	kg
Materials/fuels		
Polyethylene terephthalate, granulate, amorphous, recycled {EU without Switzerland}| polyethylene terephthalate production, granulate, amorphous, recycled | Cut-off, U	0	Kg
Polyethylene terephthalate, granulate, bottle grade {RER}| polyethylene terephthalate production, granulate, bottle grade | Cut-off, U	0	Kg
Electricity/heat		
Polymer foaming {RER}| polymer foaming | Cut-off, U	0	kg
Transport, freight, lorry 16-32 metric ton, EURO4 {RER}| market for	0	kgkm
Final waste flows		
Waste to treatment		
Waste polyethylene {RoW}| treatment of waste polyethylene, sanitary landfill | Cut-off, U	0.325	kg
Waste polyethylene {RoW}| treatment of waste polyethylene, municipal incineration | Cut-off, U	0.311	kg
Products		
TH20_Aprilia	**1**	**m2**
Materials/fuels		
100 recycled steel Aprilia	6.75	kg
Recycled 0 steel (ND) Aprilia	0.3	kg
Electrowelded mesh Aprilia	3.59	kg
Dismantling oil Aprilia	0.134*0.86	kg
cement 42,5 R II A Aprilia	52.283	kg
Gravel Aprilia	11.149+74.323	kg
Sand Aprilia	139.549	kg
Water	23.707	kg
Fluidifier Aprilia	0.378*1.06	kg
Filler Aprilia	0	kg
PET Aprilia	2.88	kg
Accelerator	0.769*1.10	kg
Products		
TH20_Bastia Umbra	**1**	**m2**
Materials/fuels		
100% Recycled Steel Bastia Umbra	3.506+1.650+0.174	kg
Recycled 0 steel (ND) Bastia Umbra	0.051+0.173+0.004	kg
Electrowelded mesh Bastia Umbra	3.751	kg

(*continued on next page*)

(*continued*)

PRODUCTS	Input	Unit
Dismantling oil Bastia Umbra	0.134*0.86	kg
cement 42,5 R II A Bastia Umbra	49.461	kg
Gravel Bastia Umbra	62.521+38.513	kg
Sand Bastia Umbra	119.319+23.202	kg
Water	24.453	kg
FluidifierBastia Umbra	0.662*1.06	kg
Filler Bastia Umbra	14.449	kg
PET Bastia Umbra	2.443	kg
Accelerator	0	kg
Products		
TH30_Aprilia	**1**	**m2**
Materials/fuels		
100% recycled steel Aprilia	12.52	kg
Recycled 0 steel (ND) Aprilia	0.556	kg
Electrowelded mesh Aprilia	5.68	kg
Dismantling oil Aprilia	0.13*0.86	kg
cement 42,5 R II A Aprilia	68.36	kg
Gravel Aprilia	14.949+97.42	kg
Sand Aprilia	182.919	kg
Water	31.07	kg
Fluidifier Aprilia	0.496*1.06	kg
Filler Aprilia	0	kg
PET Aprilia	5.28	kg
Accelerator	1.008*1.1	kg
Products		
TH30_Bastia Umbra	**1**	**m2**
Materials/fuels		
100% recycled steel Bastia Umbra	5.077+2.388+0.252	kg
Recycled 0 steel (ND) Bastia Umbra	0.074+0.005+0.250	kg
Electrowelded mesh Bastia Umbra	4.21	kg
Dismantling oil Bastia Umbra	0.11*0.86	kg
cement 42,5 R II A Bastia Umbra	53.86	kg
Gravel Bastia Umbra	62.531+48.471	kg
Sand Bastia Umbra	130.251+25.827	kg
Water	26.325	kg
Fluidifier Bastia Umbra	0.716*1.06	kg
Filler Bastia Umbra	15.538	kg
PET Bastia Umbra	5.97	kg
Accelerator	0	kg
Project Input parameters		
consumption_fuel_demolition_TH20	0.5	Undef.
consumption_fuel_demolition_TH30	0.75	Undef.

References

[1] J. Hong, G.Q. Shen, Y. Feng, W.S.T. Lau, C. Mao, Greenhouse gas emissions during the construction phase of a building: A case study in China, J. Clean. Prod. 103 (2015) 249–259, https://doi.org/10.1016/j.jclepro.2014.11.023.

[2] Global Alliance for Buildings and Construction, International Energy Agency, United Nations Environment Programme. 2019 Global Status Report for Buildings and Construction: Towards a zero-emissions, efficient and resilient buildings and construction sector. 2019.

[3] N.M. Aly, H.S. Seddeq, K. Elnagar, T. Hamouda, Acoustic and thermal performance of sustainable fiber reinforced thermoplastic composite panels for insulation in buildings, J. Build. Eng. (2021) 40, https://doi.org/10.1016/j.jobe.2021.102747.

[4] P. Santos, L. Sousa, L. Godinho, J.R. Correia, A.M.P.G. Dias, Acoustic and thermal behaviour of cross-insulated timber panels, J. Build. Eng. (2021) 44, https://doi.org/10.1016/j.jobe.2021.103309.

[5] C. Buratti, E. Belloni, E. Lascaro, F. Merli, P. Ricciardi, Rice husk panels for building applications: Thermal, acoustic and environmental characterization and comparison with other innovative recycled waste materials, Constr. Build. Mater. 171 (2018) 338–349, https://doi.org/10.1016/j.conbuildmat.2018.03.089.

[6] M. Ouakarrouch, S. Bousshine, A. Bybi, N. Laaroussi, M. Garoum, Acoustic and thermal performances assessment of sustainable insulation panels made from cardboard waste and natural fibers, Appl. Acoust. 199 (2022) 109007, https://doi.org/10.1016/j.apacoust.2022.109007.

[7] M.U. Hossain, C.S. Poon, I.M.C. Lo, J.C.P. Cheng, Comparative environmental evaluation of aggregate production from recycled waste materials and virgin sources by LCA, Resour. Conserv. Recycl. 109 (2016) 67–77, https://doi.org/10.1016/j.resconrec.2016.02.009.

[8] E. Ganjian, M. Khorami, A.A. Maghsoudi, Scrap-tyre-rubber replacement for aggregate and filler in concrete, Constr. Build. Mater. 23 (2009) 1828–1836, https://doi.org/10.1016/j.conbuildmat.2008.09.020.

[9] M.Y. Durgun, Experimental research on gypsum-based mixtures containing recycled roofing tile powder at ambient and high temperatures, Constr. Build. Mater. 285 (2021) 122956, https://doi.org/10.1016/j.conbuildmat.2021.122956.

[10] D. Robert, E. Baez, S. Setunge, A new technology of transforming recycled glass waste to construction components, Constr. Build. Mater. 313 (2021) 125539, https://doi.org/10.1016/j.conbuildmat.2021.125539.

[11] A. Arulrajah, E. Yaghoubi, Y.C. Wong, S. Horpibulsuk, Recycled plastic granules and demolition wastes as construction materials: Resilient moduli and strength characteristics, Constr. Build. Mater. 147 (2017) 639–647, https://doi.org/10.1016/j.conbuildmat.2017.04.178.

[12] Bolden, Utilization of recycled and waste materials in various construction applications, Am. J. Environ. Sci. 9 (2013) 14–24, https://doi.org/10.3844/ajessp.2013.14.24.

[13] J.K. Appiah, V.N. Berko-Boateng, T.A. Tagbor, Use of waste plastic materials for road construction in Ghana, Case Stud. Constr. Mater. 6 (2017) 1–7, https://doi.org/10.1016/j.cscm.2016.11.001.

[14] A. Mohammadinia, Y.C. Wong, A. Arulrajah, S. Horpibulsuk, Strength evaluation of utilizing recycled plastic waste and recycled crushed glass in concrete footpaths, Constr. Build. Mater. 197 (2019) 489–496, https://doi.org/10.1016/j.conbuildmat.2018.11.192.

[15] J. Thorneycroft, J. Orr, P. Savoikar, R.J. Ball, Performance of structural concrete with recycled plastic waste as a partial replacement for sand, Constr. Build. Mater. 161 (2018) 63–69, https://doi.org/10.1016/j.conbuildmat.2017.11.127.

[16] S. Agyeman, N.K. Obeng-Ahenkora, S. Assiamah, G. Twumasi, Exploiting recycled plastic waste as an alternative binder for paving blocks production, Case Stud. Constr. Mater. 11 (2019) e00246.

[17] E. Tian, J. Mo, Toward energy saving and high efficiency through an optimized use of a PET coarse filter: The development of a new electrostatically assisted air filter, Energ. Build. 186 (2019) 276–283, https://doi.org/10.1016/j.enbuild.2019.01.021.

[18] M.I.H. Hassan, A.A. Kadir, I.S.I. Arzlan, M.R.M. Tomari, N.A. Mardi, M.F. Hassan, et al., Recycling of PET bottles into different types of building materials: A review, Arch. Metall. Mater. (2023), https://doi.org/10.24425/amm.2022.137488.

[19] H. Limami, I. Manssouri, K. Cherkaoui, A. Khaldoun, Study of the suitability of unfired clay bricks with polymeric HDPE & PET wastes additives as a construction material, J. Build. Eng. 27 (2020) 100956, https://doi.org/10.1016/j.jobe.2019.100956.
[20] J.O. Akinyele, U.T. Igba, B.G. Adigun, Effect of waste PET on the structural properties of burnt bricks, Sci. Afr. 7 (2020) e00301, https://doi.org/10.1016/j.sciaf.2020.e00301.
[21] F.I. Aneke, B.O. Awuzie, M.M.H. Mostafa, C. Okorafor, Durability assessment and microstructure of high-strength performance bricks produced from PET waste and foundry sand, Materials (Basel) 14 (2021) 5635, https://doi.org/10.3390/ma14195635.
[22] A.F. Ikechukwu, C. Shabangu, Strength and durability performance of masonry bricks produced with crushed glass and melted PET plastics, Case Stud. Constr. Mater. 14 (2021) e00542, https://doi.org/10.1016/j.cscm.2021.e00542.
[23] J.A. Paschoalin Filho, J.H. Storopoli, A.J. Guerner Dias, Evaluation of compressive strength and water absorption of soilcement bricks manufactured with addition of pet (polyethylene terephthalate) wastes, Acta Sci. (2016) 38.
[24] K. Nováková, K. Šeps, H. Achten, Experimental development of a plastic bottle usable as a construction building block created out of polyethylene terephthalate: Testing PET(b)rick 1.0, J. Build. Eng. 12 (2017) 239–247, https://doi.org/10.1016/j.jobe.2017.05.015.
[25] C. Jm, M. Di, R. Sm, PET bottles for eco-friendly building in sustainable development, Int. J. Curr. Trends Eng. Res. 2 (2016) 318–326.
[26] M. Garrido, J.R. Correia, T. Keller, Effects of elevated temperature on the shear response of PET and PUR foams used in composite sandwich panels, Constr. Build. Mater. 76 (2015) 150–157, https://doi.org/10.1016/j.conbuildmat.2014.11.053.
[27] H. Xie, C. Shen, H. Fang, J. Han, W. Cai, Flexural property evaluation of web reinforced GFRP-PET foam sandwich panel: Experimental study and numerical simulation, Compos. B Eng. 234 (2022) 109725, https://doi.org/10.1016/j.compositesb.2022.109725.
[28] M. Xanthos, R. Dhavalikar, V. Tan, S. Dey, U. Yilmazer, Properties and applications of sandwich panels based on PET foams, J. Reinf. Plast. Compos. (2001).
[29] K.S. Rebeiz, Time-temperature properties of polymer concrete using recycled PET, Cem. Concr. Compos. 17 (1995) 119–124, https://doi.org/10.1016/0958-9465(94)00004-I.
[30] B. Sarde, Y. Patil, B. Dholakiya, V. Pawar, Effect of calcined kaolin clay on mechanical and durability properties of pet waste-based polymer mortar composites, Constr. Build. Mater. 318 (2022) 126027, https://doi.org/10.1016/j.conbuildmat.2021.126027.
[31] K.S. Rebeiz, Precast use of polymer concrete using unsaturated polyester resin based on recycled PET waste, Constr. Build. Mater. 10 (1996) 215–220, https://doi.org/10.1016/0950-0618(95)00088-7.
[32] S. Fadhil, M. Yaseen, The production of economical precast concrete panels reinforced by waste plastic fibers, Am. J. Civ. Eng. Arch. 3 (2015) 80–85, https://doi.org/10.12691/ajcea-3-3-4.
[33] H. Sharma, Innovative and sustainable application of PET bottle a green construction overview, Indian J. Sci. Technol. 10 (2017) 1–6, https://doi.org/10.17485/ijst/2017/v10i16/114307.
[34] A. Munir, M. Irfandi, Abdullah, A preliminary study on the use of PET bottle waste as the green roof drainage layer for thermal insulator, IOP Conf. Ser. Earth Environ. Sci. (2021) 881, https://doi.org/10.1088/1755-1315/881/1/012054.
[35] A. Briga-Sá, L. Ferreira, B. Paulo, I. Bentes, C.A. Teixeira, Energy and environmental performance assessment of reused PET bottles panels for building thermal insulation solutions, Energ. Build. 298 (2023) 113529, https://doi.org/10.1016/j.enbuild.2023.113529.
[36] A. Vargas, B.V. Silva, M.R. Rocha, F. Pelisser, Precast slabs using recyclable packaging as flooring support elements, J. Clean. Prod. 66 (2014) 92–100, https://doi.org/10.1016/j.jclepro.2013.10.059.
[37] I.A. Santana, D. Susanto, W. Widyarko, Pet plastic bottle waste with reuse approach as interior pre-fabrication modules for interior wall, Insist 2 (2017) 26, https://doi.org/10.23960/ins.v2i1.29.
[38] A.F. Abd Rashid, S. Yusoff, A review of life cycle assessment method for building industry, Renew. Sustain. Energy Rev. 45 (2015) 244–248, https://doi.org/10.1016/j.rser.2015.01.043.
[39] M. Bahramian, K. Yetilmezsoy, Life cycle assessment of the building industry: An overview of two decades of research (1995–2018), Energ. Build. (2020) 219, https://doi.org/10.1016/j.enbuild.2020.109917.
[40] C. Ingrao, A. Lo Giudice, C. Tricase, R. Rana, C. Mbohwa, V. Siracusa, Recycled-PET fibre based panels for building thermal insulation: Environmental impact and improvement potential assessment for a greener production, Sci. Total Environ. 493 (2014) 914–929, https://doi.org/10.1016/j.scitotenv.2014.06.022.
[41] F. Intini, S. Kühtz, Recycling in buildings: an LCA case study of a thermal insulation panel made of polyester fiber, recycled from post-consumer PET bottles, Int. J. Life Cycle Assess. 16 (2011) 306–315, https://doi.org/10.1007/s11367-011-0267-9.
[42] X. Yang, M. Huang, F. Lin, Research strategies on new prefabricated technology for underground metro stations, Urban Rail Transit. 5 (2019) 145–154, https://doi.org/10.1007/s40864-019-0106-z.
[43] W. Lu, W.M.W. Lee, F. Xue, J. Xu, Revisiting the effects of prefabrication on construction waste minimization: A quantitative study using bigger data, Resour. Conserv. Recycl. 170 (2021) 105579, https://doi.org/10.1016/j.resconrec.2021.105579.
[44] S. Lehmann, Low carbon construction systems using prefabricated engineered solid wood panels for urban infill to significantly reduce greenhouse gas emissions, Sustain. Cities Soc. 6 (2013) 57–67, https://doi.org/10.1016/j.scs.2012.08.004.
[45] A. Carbonari, M. De Grassi, C. Di Perna, P. Principi, Numerical and experimental analyses of PCM containing sandwich panels for prefabricated walls, Energ. Build. 38 (2006) 472–483, https://doi.org/10.1016/j.enbuild.2005.08.007.
[46] V. Puri, P. Chakrabortty, S. Anand, S. Majumdar, Bamboo reinforced prefabricated wall panels for low cost housing, J. Build. Eng. 9 (2017) 52–59, https://doi.org/10.1016/j.jobe.2016.11.010.
[47] R. O'Hegarty, A. Reilly, R. West, O. Kinnane, Thermal investigation of thin precast concrete sandwich panels, J. Build. Eng. 27 (2020) 100937, https://doi.org/10.1016/j.jobe.2019.100937.
[48] L. Peng, L. Xiaoyong, C. Ying, Y. Zhiwu, Y. Dayou, Thermodynamic and acoustic behaviors of prefabricated composite wall panel, Structures 28 (2020) 1301–1313, https://doi.org/10.1016/j.istruc.2020.09.069.
[49] G.K. Oral, A.K. Yener, N.T. Bayazit, Building envelope design with the objective to ensure thermal , visual and acoustic comfort conditions 39 (2004) 281–287. https://doi.org/10.1016/S0360-1323(03)00141-0.
[50] L. Huang, Y. Zhu, Q. Ouyang, B. Cao, A study on the effects of thermal, luminous, and acoustic environments on indoor environmental comfort in offices, Build. Environ. 49 (2012) 304–309, https://doi.org/10.1016/j.buildenv.2011.07.022.
[51] E.L. Krüger, P.H.T. Zannin, Acoustic, thermal and luminous comfort in classrooms, Build. Environ. 39 (2004) 1055–1063, https://doi.org/10.1016/j.buildenv.2004.01.030.
[52] R. Hufenus, Y. Yan, M. Dauner, T. Kikutani, Melt-spun fibers for textile applications, Materials (Basel) 13 (2020) 4298, https://doi.org/10.3390/ma13194298.
[53] A.L. Pisello, F. Cotana, A. Nicolini, C. Buratti, Effect of dynamic characteristics of building envelope on thermal-energy performance in winter conditions: In field experiment, Energ. Build. 80 (2014) 218–230, https://doi.org/10.1016/j.enbuild.2014.05.017.
[54] ASTM E2611-17: Standard Test Method for Normal Incidence Determination of Porous Material Acoustical Properties Based on the Transfer Matrix Method. n.d.
[55] International Organization for Standardization. ISO 10534-2: 2001: Acoustics-Determination of Sound Absorption Coefficient and Impedance in Impedance Tubes. 2001.
[56] ISO 16283-3:2016: Acoustics — Field measurement of sound insulation in buildings and of building elements — Part 3: Façade sound insulation. n.d.
[57] ISO 354:2003: Acoustics — Measurement of sound absorption in a reverberation room. n.d.
[58] ISO 3382-2:2008: Acoustics — Measurement of room acoustic parameters — Part 2: Reverberation time in ordinary rooms. n.d.
[59] UNI EN ISO 717-1:2021: Acoustics - Rating of sound insulation in buildings and of building elements - Part 1: Airborne sound insulation. n.d.
[60] ISO 22007-2: Plastics — Determination of thermal conductivity and thermal diffusivity — Part 2: Transient plane heat source (hot disc) method. 2015.
[61] ISO 9869-1:2014: Thermal insulation -Building elements - In-situ measurement of thermal resistance and thermal transmittance - Part 1: Heat flow meter method. n. d.
[62] ISO 14021:2016: Environmental labels and declarations - Self-declared environmental claims (Type II environmental labelling). n.d.
[63] EN ISO 14020:2001: Environmental labels and declarations - General principles. n. d.
[64] ISO 14040:2006: Environmental management — Life cycle assessment — Principles and framework. n.d.
[65] ISO 14044:2021: Environmental management - Life cycle assessment - Requirements and guidelines n.d.
[66] EN 15804:2012+A2:2019: Sustainability of construction works - Environmental product declarations - Core rules for the product category of construction products. n.d.
[67] A. Gupta, and R. Sharma, "A New Method for Estimation of Automobile Fuel Adulteration", in Air Pollution. London, United Kingdom: IntechOpen, 2010 [Online]. Available: https://www.intechopen.com/chapters/11778 doi: 10.5772/10054 n.d.
[68] Fondazione per lo sviluppo sostenibile, FISE UNICIRCULAR - Unione Imprese Economia Circolare. L'Italia del Riciclo 2020. 2020.
[69] ISPRA. Rapporto Rifiuti Urbani - Edizione 2021. n.d.
[70] M.S.M. Noh, Z. Ahmad, A. Ibrahim, P. Walker, Development of new prefabricated wall constructed using wood-wool cement composite panel, Procedia Environ. Sci. 34 (2016) 298–308, https://doi.org/10.1016/j.proenv.2016.04.027.
[71] R. Garay, F. Pfenniger, M. Castillo, C. Fritz, Quality and Sustainability indicators of the prefabricated wood housing industry—A Chilean case study, Sustainability 13 (2021) 8523, https://doi.org/10.3390/su13158523.
[72] S. Zou, H. Li, S. Wang, R. Jiang, J. Zou, X. Zhang, et al., Experimental research on an innovative sawdust biomass-based insulation material for buildings, J. Clean. Prod. 260 (2020) 121029, https://doi.org/10.1016/j.jclepro.2020.121029.
[73] A.L. Pisello, C. Piselli, F. Cotana, Influence of human behavior on cool roof effect for summer cooling, Build. Environ. (2015), https://doi.org/10.1016/j.buildenv.2014.09.025.